THE UNIVERSITY OF MANITOBA

A LOCAL MODE DESCRIPTION OF THE CH-STRETCHING OVERTONE SPECTRA OF THE ALKANES

by

WAYNE R. A. GREENLAY

A THESIS
SUBMITTED TO THE FACULTY OF GRADUATE STUDIES
IN PARTIAL FULFILMENT OF THE REQUIREMENTS FOR THE DEGREE
OF MASTER OF SCIENCE

DEPARTMENT OF CHEMISTRY

WINNIPEG, MANITOBA
MAY, 1978

A LOCAL MODE DESCRIPTION OF THE CH-STRETCHING OVERTONE SPECTRA OF THE ALKANES

BY

WAYNE R.A. GREENLAY

A dissertation submitted to the Faculty of Graduate Studies of the University of Manitoba in partial fulfillment of the requirements of the degree of

MASTER OF SCIENCE

©1978

Permission has been granted to the LIBRARY OF THE UNIVERSITY OF MANITOBA to lend or sell copies of this dissertation, to the NATIONAL LIBRARY OF CANADA to microfilm this dissertation and to lend or sell copies of the film, and UNIVERSITY MICROFILMS to publish an abstract of this dissertation.

The author reserves other publication rights, and neither the dissertation nor extensive extracts from it may be printed or otherwise reproduced without the author's written permission.

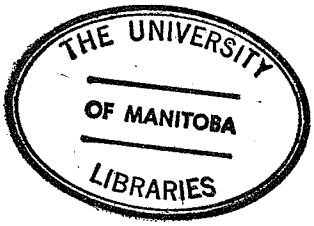

ACKNOWLEDGEMENTS

I would like to dedicate this work to my wife, Jill, and to my parents in recognition of their invaluable support throughout the duration of my studies. I would like to express my gratitude to Dr. Bryan Henry, not only for his assistance and advice on my project, but more importantly, for his patience with an often frustrating student. Also, I would like to acknowledge the contribution of the computer programs by Dr. R. N. Jones of NRC, Ottawa and thank NRC, the University of Manitoba and the Chemistry Department for financial support.

ABSTRACT

The overtone spectra of the normal alkanes, propane to n-heptane, and several branched alkanes are measured in the liquid or gas phase from 6000 to 15000 Å. Each overtone band is principally composed of peaks corresponding to the different CH oscillator types in the molecule, CH_3, CH_2 or CH. The localized character of the overtone bands increases with increasing energy. The relative intensity of the CH_2 peak to the CH_3 peak correlates with the number of CH_2 hydrogens in the molecule. Combination bands involving CH local modes and a lower frequency normal mode are identified. The relative intensities of the components of these bands parallels that of the pure CH-stretching overtone bands. Combination bands between different CH-stretching local modes are also observed and tentatively assigned. Deconvolution of the main overtone bands for $\Delta v_{CH} = 3$, 4 and 5 of the normal alkane spectra gives further information about individual local mode peaks, particularly with regard to bandshape and bandwidth. The local mode frequencies, ω_1, and diagonal local mode anharmonicity constants, X_{11}, for the molecules are obtained from a local mode analysis of both the observed spectral data and deconvolution results. These two parameters form consistent sets for a given CH oscillator type. The CH-stretching overtone spectra of 3-methylpentane are measured for both the liquid and low temperature (77°K glass) solid phases. Calculated diagonal local mode anharmonicity constants show that the local vibrational potential is more harmonic at high viscosity.

TABLE OF CONTENTS

	Page
ACKNOWLEDGEMENTS	i
ABSTRACT	ii
TABLE OF CONTENTS	iii
LIST OF FIGURES	v
LIST OF TABLES	viii
INTRODUCTION	1
EXPERIMENTAL	9
i) Solids	9
ii) Liquids	9
iii) Gases	10
iv) General Procedures	11
RESULTS	13
DISCUSSION	59
A) The Local Mode Character of CH-Stretching Overtone Spectra	59
i) Nonequivalent CH Groups	59
ii) Other Local Mode Characteristics	61
B) DCON--The Deconvolution Study	66
i) Bandwidths	66
ii) Local Mode CH-CH Combination Bands	68
iii) Peak Separation	70

Page

C) Anharmonicity Constants 73

i) The Morse Oscillator 73

ii) Dissociation Energies 74

iii) Medium Effects 75

APPENDIX 79

i) Cyclohexane 79

ii) Bandshapes 80

BIBLIOGRAPHY 82

LIST OF FIGURES

Figure		Page
1	The overtone spectrum of gas phase propane at room temperature in the region of $\Delta v_{CH} = 3$	16
2	The overtone spectrum of gas phase n-butane at room temperature in the region of $\Delta v_{CH} = 3$	17
3	The overtone spectrum of liquid phase n-pentane at room temperature in the region of $\Delta v_{CH} = 3$	18
4	The overtone spectrum of liquid phase n-hexane at room temperature in the region of $\Delta v_{CH} = 3$	19
5	The overtone spectrum of liquid phase n-heptane at room temperature in the region of $\Delta v_{CH} = 3$	20
6	The overtone spectrum of liquid phase 2-methylbutane at room temperature in the region of $\Delta v_{CH} = 3$	21
7	The overtone spectrum of liquid phase 3-methylpentane at room temperature in the region of $\Delta v_{CH} = 3$	22
8	The overtone spectrum of liquified propane at room temperature in the region of $\Delta v_{CH} = 4$	23
9	The overtone spectrum of liquified n-butane at room temperature in the region of $\Delta v_{CH} = 4$	24
10	The overtone spectrum of liquid phase n-pentane at room temperature in the region of $\Delta v_{CH} = 4$	25
11	The overtone spectrum of liquid phase n-hexane at room temperature in the region of $\Delta v_{CH} = 4$	26
12	The overtone spectrum of liquid phase n-heptane at room temperature in the region of $\Delta v_{CH} = 4$	27
13	The overtone spectrum of liquified isobutane at room temperature in the region of $\Delta v_{CH} = 4$	28
14	The overtone spectrum of liquid phase 2-methylbutane at room temperature in the region of $\Delta v_{CH} = 4$	29
15	The overtone spectrum of liquid phase 3-methylpentane at room temperature in the region of $\Delta v_{CH} = 4$	30
16	The overtone spectrum of liquid phase cyclohexane at room temperature in the region of $\Delta v_{CH} = 4$	31

Figure Page

17 The overtone spectrum of liquified propane at room temperature in the region of $\Delta v_{CH} = 5$ and $\Delta v_{CH} = 6$ 32

18 The overtone spectrum of liquified n-butane at room temperature in the region of $\Delta v_{CH} = 5$ and $\Delta v_{CH} = 6$ 33

19 The overtone spectrum of liquid phase n-pentane at room temperature in the region of $\Delta v_{CH} = 5$ and $\Delta v_{CH} = 6$ 34

20 The overtone spectrum of liquid phase n-hexane at room temperature in the region of $\Delta v_{CH} = 5$ and $\Delta v_{CH} = 6$ 35

21 The overtone spectrum of liquid phase n-heptane at room temperature in the region of $\Delta v_{CH} = 5$ and $\Delta v_{CH} = 6$ 36

22 The overtone spectrum of liquified isobutane at room temperature in the region of $\Delta v_{CH} = 5$ and $\Delta v_{CH} = 6$ 37

23 The overtone spectrum of liquid phase 2-methylbutane at room temperature in the region of $\Delta v_{CH} = 5$ and $\Delta v_{CH} = 6$. . . 38

24 The overtone spectrum of liquid phase 3-methylpentane at room temperature in the region of $\Delta v_{CH} = 5$ and $\Delta v_{CH} = 6$. . . 39

25 The overtone spectrum of liquid phase cyclohexane at room temperature in the region of $\Delta v_{CH} = 5$ and $\Delta v_{CH} = 6$ 40

26 An illustration of the calculated local mode components of the $\Delta v_{CH} = 3$, CH-stretching overtone band of n-heptane . . . 43

27 An illustration of the calculated local mode components of the $\Delta v_{CH} = 4$, CH-stretching overtone band of n-heptane . . . 44

28 An illustration of the calculated local mode components of the $\Delta v_{CH} = 5$, CH-stretching overtone band of n-heptane . . . 45

29 An illustration of the calculated local mode components of the $\Delta v_{CH} = 4$, CH-stretching overtone band of isobutane . . . 46

30 Calculated and observed CH-stretching overtone band of n-heptane corresponding to $\Delta v_{CH} = 5$. 47

31 A plot of Equation 2 for the CH_3 transitions from the experimental solid (77°K glass) and liquid (room temperature) spectra of 3-methylpentane in the region $\Delta v_{CH} = 3$ to $\Delta v_{CH} = 6$ 54

32 Calculated and observed $\Delta v_{CH} = 4$, CH-stretching overtone spectra of dichloromethane, taken from Figure 5 of reference 4, copyright Academic Press 62

Figure Page

33 The more harmonic potential curve, resulting from the solid matrix perturbation of the original Morse potential for the liquid phase 76

LIST OF TABLES

Table		Page
1	The observed band maxima for the CH-stretching overtone spectra of several alkanes	41
2	Data obtained from the deconvolution of the CH-stretching overtone bands, Δv_{CH} = 3, 4 and 5, of some alkanes	48
3	Separation of the CH_3 and CH_2 peaks for the alkane overtones	51
4	Results of CH_3 anharmonicity calculations from observed CH_3 peak maxima	52
5	Results of the CH_3 and CH_2 anharmonicity calculations from the deconvoluted peak maxima	54
6	A comparison of calculated and literature dissociation energies for CH_3 and CH_2 type C-H bonds	55
7	Diagonal local mode anharmonicity constants for the CH_3 transitions in 3-methylpentane	58

INTRODUCTION

The local mode model has been previously developed (1, 2, 3, 4) to interpret the spectra of highly vibrationally excited molecules. Normal modes, although suitable for the understanding of the fundamental and lower overtone regions of infra-red spectra, have been shown to be inadequate in the description of the higher overtone regions. For example, CH-stretching overtone spectra calculated for dichloromethane, on the basis of anharmonically coupled normal modes, were found to be too complex and resultant bandwidths too large in comparison to the experimentally observed spectra. In that study (4), a general local mode theory was presented and it was concluded that the most prominent spectral features of CH-stretching overtone spectra corresponded to localized modes of vibration, that is, multiple excitation of a single CH oscillator. Many organic molecules contain CH oscillators, however, this study deals specifically with the CH-stretching overtone spectra of the alkanes. Reasons for this choice are outlined later in the Introduction.

The infra-red spectra of the alkanes and their analysis are well documented in the literature (see, for example, references 5, 6, 7 and 8). One of the more important of these studies is the extensive normal mode analysis of the n-alkanes by Snyder and collaborators (8). More relevant to this work is the presentation by Avanessoff and Gaumann of a group model and its application to the analysis of the C-H/C-D valence vibrations of some alkanes (9, 10). The authors employ an experimental model of group frequencies, for methyl and methylene groups, to aid in the assignment of the frequencies.

Only a limited amount of work has been devoted to the CH-stretching overtone spectra of these alkanes. Most recently, the CH-stretching overtone spectra of methane and ethane were interpreted in terms of local modes (11). Prior to that publication was the documentation of the extension of the previously mentioned group model of Avanessoff and collaborators to the observed first and second overtone (Δv_{CH} = 2 and 3) spectra of the valence C-H vibrations of alkanes (12). The higher overtones, out to $\Delta v_{CH} = 6$, were only measured for n-hexane. This later article is particularly interesting. Calculations, based on a normal mode analysis of the valence C-H vibrations of isolated methyl and methylene groups, are compared to observed overtone frequencies. Even this group model, which takes into account the dependence of the observed spectral structure on the CH_3 and CH_2 groups of the molecule, a concept discussed later in this report, is acknowledged by the authors to fail as low as $\Delta v_{CH} = 3$ to adequately represent the CH-stretching overtone spectra.

The present study comprises a further look at the local-mode character of these CH-stretching overtone spectra. By local mode character I mean the spectral features which have been shown, in the aforementioned paper on dichloromethane (4), to be more readily interpreted in terms of local modes. Before introducing other aspects of this work, a summary of several of the more important characteristics will be given.

The simplicity of CH-stretching overtone spectra has been observed for a wide variety of compounds, including smaller molecules such as dichloromethane (4) and even larger aromatic systems such as naphthalene

(13). It appears that only the most anharmonic normal mode components, that is the ones which correspond to multiple excitation of a single local oscillator, are observed in the higher overtone regions. The highest frequency normal mode components dõonot seem to contribute at all, which is the reason that the bands are simpler and narrower than expected. The simplicity is not uniform for all overtones, but has been observed to increase with an increase in the vibrational quantum number, v. A normal mode analysis would predict the opposite effect due to an increasing number of symmetry allowed normal mode components.

Although, the pure local mode overtones are the most intense spectral features, combination bands of much less intensity do occur. Two types of combination bands have been previously identified and both are observed to increase in importance for the lower overtones. Indeed, the observed increase in complexity of the lower overtones is largely due to this increase in importance and intensity of these combination bands.

The first type, local mode CH-CH combination bands, appear immediately to the high energy side of a pure local mode overtone band. These local mode CH-CH combination bands are the result of a division of the vibrational quanta among two CH bonds. In local mode terms, such bands are said to be combination bands involving two CH local modes and demonstrate the existence of a small coupling between local modes. However, these local mode CH-CH combination bands can also be interpreted to represent the manifestations of a normal mode pattern in CH-stretching overtones. The other type of combination band is the result of a more direct influence of normal modes on these overtones. This second type

of combination band appears to even higher energy relative to the pure local mode overtone and has been assigned as a combination band between a multiply excited local CH oscillator and a single quantum of a lower frequency normal mode. Both types of combination bands are much less intense and decrease much faster in intensity than related pure local mode overtones, such that by $\Delta v_{CH} = 5$ only a slight broadening of the high energy side of the pure local mode overtone, the result of local mode CH-CH combination activity, is observed.

For $\Delta v_{CH} = 3$ overtones, a much greater influence of normal modes has generally been observed. In the $\Delta v_{CH} = 4$ and 5 regions, the band structures can be described in terms of pure local mode overtones and the two types of combination bands. However, the increased complexity, previously observed in $\Delta v_{CH} = 3$ bands, suggests that normal modes contribute significantly for this overtone. Recent work on the overtone spectra of the dihalomethanes (14) has corroborated a previous report by Wallace (15), which indicates that the extent of this normal mode influence, and conversely the applicability of a local mode analysis, is dependent on the mass difference between hydrogen and the moiety to which it is bound.

The alkanes were chosen for this study for several reasons other than availability. Alkanes contain a relative abundance of CH oscillators, which aid in the problem of weak intensities encountered in the overtone region. More importantly, several types of CH oscillator, that is CH_3, CH_2 and CH, are found in saturated alkanes. The presence of several different CH oscillator types was desired for a further study of another local mode characteristic, the effect of nonequivalent CH

groups.

The effect of nonequivalent CH groups was previously observed in the CH-stretching overtone spectra of benzene, toluene and the xylenes (11). In the benzene spectra, a single peak was observed for each overtone and represented the six equivalent aryl CH bonds. However for toluene and the xylenes, a second peak is resolved to the low energy side of the aryl peak. It appears at an energy comparable to a corresponding transition in ethane and therefore can be identified with an alkyl CH local mode. Thus it has been observed that nonequivalent CH groups are resolved in the overtone region as distinct peaks, reflecting the differences in the nature of the nonequivalent CH bonds. The narrow bandwidths, observed for local mode bands, are instrumental in the resolution of these peaks. However, the difference between the primary, secondary and tertiary CH oscillators of the alkanes (CH_3, CH_2 and CH groups, respectively) is much less than that between aryl and alkyl CH groups. Therefore, the possible resolution of these CH oscillators was another purpose of this study.

Furthermore, a rough correlation between the number of a given type of CH oscillator and the area of the local mode overtone peak, representing that CH type, has been observed (11, 13, 16). A comparison of the overtone spectra, Δv_{CH} = 3 to 5, of toluene and benzene has shown a relative decrease in the aryl peak size of the methyl substituted benzene. A second methyl substitution results in a further decrease in the aryl peak size and an approximate doubling in the alkyl peak size in the three xylenes. A similar correlation has been reported for the $\Delta v_{CH} = 6$ overtone transitions of benzene, toluene, m-xylene and

trimethylbenzene, observed by Swofford et al. using the more sensitive technique of thermal lensing spectroscopy (13). A further investigation of the correlation is possible with the alkanes, which present numerous different combinations of three hydrogen types. The concepts of non-equivalent CH groups and the correlation of peak area to the number of a specific CH oscillator type are important for they cannot be explained in terms of normal modes.

The consistency of CH-stretching overtone spectra is another observed local mode characteristic. For example for a given CH oscillator type, corresponding overtone transitions have been observed to occur at approximately the same energy for several compounds. The bandwidths of each overtone are also essentially unchanged for a wide variety of molecules. The consistency of the overtone bands is difficult to explain in terms of normal modes because of the large difference in the predicted number of allowed states of different molecules.

The extent of the applicability of a local mode description to CH-stretching overtones was another concern of this study. To this purpose, a deconvolution[a] of experimentally recorded CH-stretching overtone spectra was performed to see how well these spectra could be constructed in terms of the sum of Lorentzian peaks, each corresponding to a different local CH oscillator. The Lorentzian shape has recently been corroborated by the "nearly perfect Lorentzian lineshape" observed in a

---

[a]Deconvolute is used throughout this text to indicate the decomposition of the overtone bands into their component peaks.

dye laser study of the Δv_{CH} = overtone of gaseous benzene (17). Furthermore, a Lorentzian lineshape is predicted for a transition, in an isolated molecule, to a discrete state, which is coupled to a manifold of nearly degenerate states (18). Here, the given state is coupled anharmonically to other vibrational modes. However, in the liquid phase, intermolecular interactions occur and the peaks broaden substantially. Therefore, there exists the possibility of non-Lorentzian lineshapes.

Deconvolution of the overtone spectra also makes possible the more accurate assignment of peak maxima, usually difficult due to the shifting of the maxima of overlapping peaks. These more accurate maxima are required for the calculation of CH-stretching diagonal local mode anharmonicity constants.

The energy of vibrational states, corresponding to the local CH oscillator, can be expressed as

$$E = E_o + \Sigma v_i \omega_i + \sum_{i>j} \Sigma c_{ij} \omega_{ij} + \sum_{i \geq j} \sum v_i v_j X_{ij} \qquad (1)$$

where v_i and ω_i are the vibrational quantum number and harmonic frequency respectively, associated with local mode i. X_{ij} is the local mode anharmonicity constant and ω_{ij} is a harmonic coupling term of the order of $(\omega_i - \omega_j)$. For a set of nearly degenerate oscillators, such as the alkyl CH oscillator types, the term $(\omega_i - \omega_j)$ is small and the harmonic coupling term can be neglected. Therefore for the excitation of a single oscillator from the vibrational ground state to the state v_i, the transition energy is simply given by

$$\Delta E = v_i \omega_i + v_i^2 X_{ii} \qquad (2)$$

A plot of $\Delta E/v_i$ versus v_i will yield, ω_i, the local mode harmonic frequency as the intercept and, X_{ii}, the local mode diagonal anharmonicity constant as the slope.

In summation, this work is divided into three areas of concern. The first section will deal solely with the experimentally obtained CH-stretching overtone spectra of some alkanes. The local mode character of these alkane overtone spectra will be discussed. Secondly, the results of the deconvolution of the spectra will be introduced. This second section will provide a more quantitative look at local mode character in CH-stretching overtone spectra and also be converned with the extent of the applicability of local modes to such spectra. Finally, CH-stretching local mode diagonal anharmonicity constants, X_{ii}'s, are calculated and discussed.

EXPERIMENTAL

Spectra were obtained for solid, liquid and gas phase samples in this study and, since each phase required specific experimental conditions, these will be discussed separately.

i) Solids

The only solid phase alkane studied was 3-methylpentane, as it forms a clear glass at 77°K. Liquid 3-methylpentane was obtained from the Phillips Petroleum Co. and purified by a modification of the method of Potts (19). For Δv_{CH} = 4, 5 and 6, the glass was contained in an 8 cm quartz cell fitted in an all quartz dewar (#203908, H. S. Martin & Co., Evanston, Illinois). However for Δv_{CH} = 3, 3-methylpentane in a 1 cm square Pyrex cell was cooled to 77°K in an Oxford Instrument DN704 optical dewar. The change of cells was necessitated by the requirement of a shorter pathlength.

The samples were cooled gradually over a period of at least one hour. It was observed that the longer pathlength samples were cloudy, probably due to residual water frozen into the glass, and this resulted in a higher background absorbance. At first density gradient filters in the reference beam were required to bring the baseline onto scale. However, it was found that if the cell was turned at a slight angle with respect to the beam, the background absorbance was considerably reduced and the filters not required. No shift in the peak maxima was observed to occur from this procedure.

ii) Liquids

The majority of the alkanes studied were liquids. The sources and purities of these chemicals were as follows: Matheson, Coleman and

Bell, spectroquality (n-hexane, n-heptane, 2-methylbutane, cyclohexane); Fisher Scientific Co., spectranalyzed (n-pentane, cyclohexane); Phillips Petroleum Co., 99 Mol % (3-methylpentane). Because of the intensity of the CH-stretching mode, the long pathlengths of neat liquid, the spectral region observed and other reasons, absorptions due to impurities were not observed and so further purification was not required. These liquid alkane samples were run as neat liquids and contained in 1 cm (Δv_{CH} = 3) and 10 cm (Δv_{CH} = 4, 5, 6) quartz cells. Measurement of the Δv_{CH} = 2 transition for 3-methylpentane required a pathlength less than 1 cm and so a 1 cm divided cell was filled only on one side of the divider. The result was an effective pathlength of approximately 0.5 cm.

iii) Gases

Several gas samples were also studied. These included propane, n-butane and isobutane and all were received from the Phillips Petroleum Co. as lecture bottles of liquified gas in excess of 99.9% in purity. The Δv_{CH} = 4, 5 and 6 results for these compounds were not acquired on the gaseous samples as originally hoped. Intentions were to use a high pressure gas cell, previously described by Hayward (20), to observe the desired transitions, but pressures of at least 1000 psi are required to obtain a measurable intensity. These samples' pressures are all less than 150 psi. The problem was overcome by effectively distilling these samples into the high pressure gas cell. The gas cylinder's temperature was raised several degrees above room temperature and upon opening the valve, the liquified gas flowed through a connecting system into the high pressure gas cell. The result was an approximately 5 cm pathlength of liquified gas, under pressure.

Recently, a long pathlength, low pressure gas cell (Wilks Scientific Corp., 20 meter variable long pathlength gas cell, Model No. 5720) became available for use. This cell was used to obtain the $\Delta v_{CH} = 3$ gas phase spectra of propane and n-butane. The pathlength for both samples was 2.25 m, but for propane some of the nitrogen, used to flush the cell, was left in the cell and a relatively reduced intensity was observed for that sample.

iv) General Procedures

All spectra were measured using a Cary 14 spectrophotometer, operated in the infra-red mode. Two slidewires were used, a 0 to 2 absorbance slidewire for $\Delta v_{CH} = 3$ and 4 and 0 to 0.2 absorbance, expanded scale slidewire for $\Delta v_{CH} = 5$ and 6. Reference samples were not used, that is the samples were referenced to air. The spectral slit width was never more than 8Å, and so is negligible when compared to the widths of the observed overtone bands.

Deconvolution studies were performed using slightly modified versions of programs PC-138 (21), PC-116 (22) and PC-122 (22) courtesy of Dr. R. N. Jones. The spectra were digitized and the results converted from wavelength in Angstroms and absorbance, to wavenumbers and transmittance, respectively by program PC-138. The data were read into PC-138 with a given wavelength spacing between the points. Since a direct conversion to wavenumbers would not result in a desired constant wavenumber interval, the authors, Jones et al. employed an interpolation algorithm, using a five point Lagrange formula, to obtain the desired interval between the output data points. The data was then ready for analysis by program PC-116.

A brief explanation of PC-116 will now be given, with an emphasis on aspects more relevant to this work. A more complete discussion for all these programs is given in references 21 and 22. Program PC-116 was written with the analysis of the infra-red spectra of condensed phase systems in mind. It is written, as are the others, in Fortran IV. The program can utilize Lorentz, Gauss, Lorentz-Gauss product or Lorentz-Gauss sum functions as required, for these bandshapes are the most probable in the infra-red spectra of liquid phase samples. PC-116 will, given a set of approximate defining parameters for each peak, an approximate baseline, the number of peaks, the desire bandshape and other input data, optimize the approximate parameters of single or multiple overlapping peaks.

A non-linear least squares method, based on algorithms by Meiron and Marquardt, is used to optimize the parameters. An equation is set up, which adjusts the parameters in iterative steps. The actual adjustments are made by matrices, whose elements are related to the partial derivatives of the differences between the observed and calculated values, f_i, with respect to each parameter, x_k, in other words $\partial f_i/\partial x_i$. Termination of the iterations will occur for several reasons. The most important is, of course, a successful fit of the data by the given function to within a specified tolerance. For this work a significant fit was achieved when the maximum ordinate difference, FM, was less the 0.001 transmittance units. A second reason is slow convergence. In fact, it was slow convergence that terminated all the deconvolutions performed in this study. Slow convergence will result if the minimization of the difference function proceeds too slowly and again is

governed by a specified tolerance limit. A check for slow convergence is performed for every iteration. The sum of the squares of the difference between the observed and calculated results, FSM, is calculated for each iteration. If the ratio of the value of FSM for the previous iteration to its present value was ever less than 1.002 than slow convergence was indicated for these deconvolution studies. If this is the reason for termination, then the optimized parameters, calculated before the tolerance limit was exceeded, are printed out. Even though slow convergence was responsible for the termination of all the deconvolutions, reasonable fits of the data were obtained. Also, although numerous fits were possible for the given data it is noted that the results achieved were physically significant. The comparison of calculated band envelopes to the experimentally observed overtones will be discussed in the results section.

In this study, a Lorentz bandshape was chosen to fit the local mode CH-stretching overtones. Three parameters, x_1, the maximum peak absorbance, x_2, the wavenumber position of the peak maximum and x_3, where $2/x_3$ is the full width at half maximum, are necessary to define a Lorentz band. A fourth parameter in the program is the baseline constant, and it is used to represent a constant background absorbance. For $\Delta v_{CH} = 3$ and 4, this constant background absorbance was able to adequately represent the observed level baseline, but for $\Delta v_{CH} = 5$ the baseline rises sharply toward higher energy. The rising baseline was found to cause difficulties in the deconvolution of the $\Delta v_{CH} = 5$ overtones and comparison of observed and calculated band envelopes revealed large differences.

Often, calculated peaks on the lower energy side of band, for example CH_2, were observed to exceed the absorbance of the experimental band envelope. The background absorbance, represented by the spectrum of carbon tetrachloride in the $\Delta v_{CH} = 5$ region, was finally measured and incorporated into the program, to be subtracted from the sample absorbance. Also, a linear baseline correction was used for $\Delta v_{CH} = 3$ of propane to account for the rising background absorbance caused by a decreasing reflectivity of the low pressure gas cell's mirrors. The baseline corrections were found to have no appreciable effect on the position of the maxima of larger peaks at higher energy, such as CH_3, but the position of smaller peaks at lower energy, such as CH, were quite sensitive to any changes in baseline.

A comparison of the experimental and calculated band envelopes was frequently done to check the quality of the fit. Once the optimum values for the parameters x_1, x_2 and x_3 were obtained, program PC-122 was used to calculate the ordinates of the band envelope. The calculated and observed band envelopes were plotted and compared visually.

Another method of comparison of the calculated and observed band envelopes was through the final calculated value of FM, the maximum ordinate difference. Values of FM and WFM, the wavenumber position of this maximum difference, were calculated and printed for every iteration of program PC-116. FM and WFM were used in conjunction with the visual comparison of experimental and calculated band envelopes to gauge and compare the results of the deconvolution program.

RESULTS

In this study the CH-stretching overtone spectra of a number of alkanes have been measured in the region $\Delta v_{CH} = 3$ to $\Delta v_{CH} = 6$. Presented here are the straight chain series of propane to n-heptane, the branched alkanes, isobutane, 2-methylbutane and 3-methylpentane (3MP) and also a ring alkane, cyclohexane. The experimental spectra are given in figures 1 through 7, 8 through 16, and 17 through 25 for the regions $\Delta v_{CH} = 3$, $\Delta v_{CH} = 4$ and $\Delta v_{CH} = 5$ and 6, respectively. With the exception of propane and n-butane, spectral intensities are effectively multiplied by 1, 10 and 100 for the $\Delta v_{CH} = 3$, 4 and 5 regions respectively, due to changed experimental conditions of cell pathlength and slidewire. $\Delta v_{CH} = 3$ spectra are not given for isobutane and cyclohexane.

The maxima for all reasonably resolved overtone bands are given in Table 1. The CH_3 type, CH-stretching overtone peak is given for all compounds, because it was well resolved for all the alkanes studied. The given values, unless indicated otherwise, are the average of at least five spectra. Representative uncertainties for the CH_3 peaks are ± 3 cm^{-1} for $\Delta v_{CH} = 3$, 4 and 5 and ± 10 cm^{-1} for $\Delta v_{CH} = 6$. In general, the CH_2 peaks are several cm^{-1} more uncertain, due to poorer resolution. The $\Delta v_{CH} = 6$ CH_3 results, for propane and n-butane, are only approximate due to extensive background noise for these samples in that region. Figure 17 illustrates exceptional noise in the region below 7000 Å for propane.

A computer assisted deconvolution of overtone bands $\Delta v_{CH} = 3$, 4 and 5 was performed for the straight chain alkanes and isobutane ($\Delta v_{CH} = 4$ and 5 only). The results of this study, in the form of the peak

Fig. 1 The overtone spectrum of gas phase (∿100 psi) propane at room temperature in the region of $\Delta v_{CH} = 3$. 2.25 m pathlength.

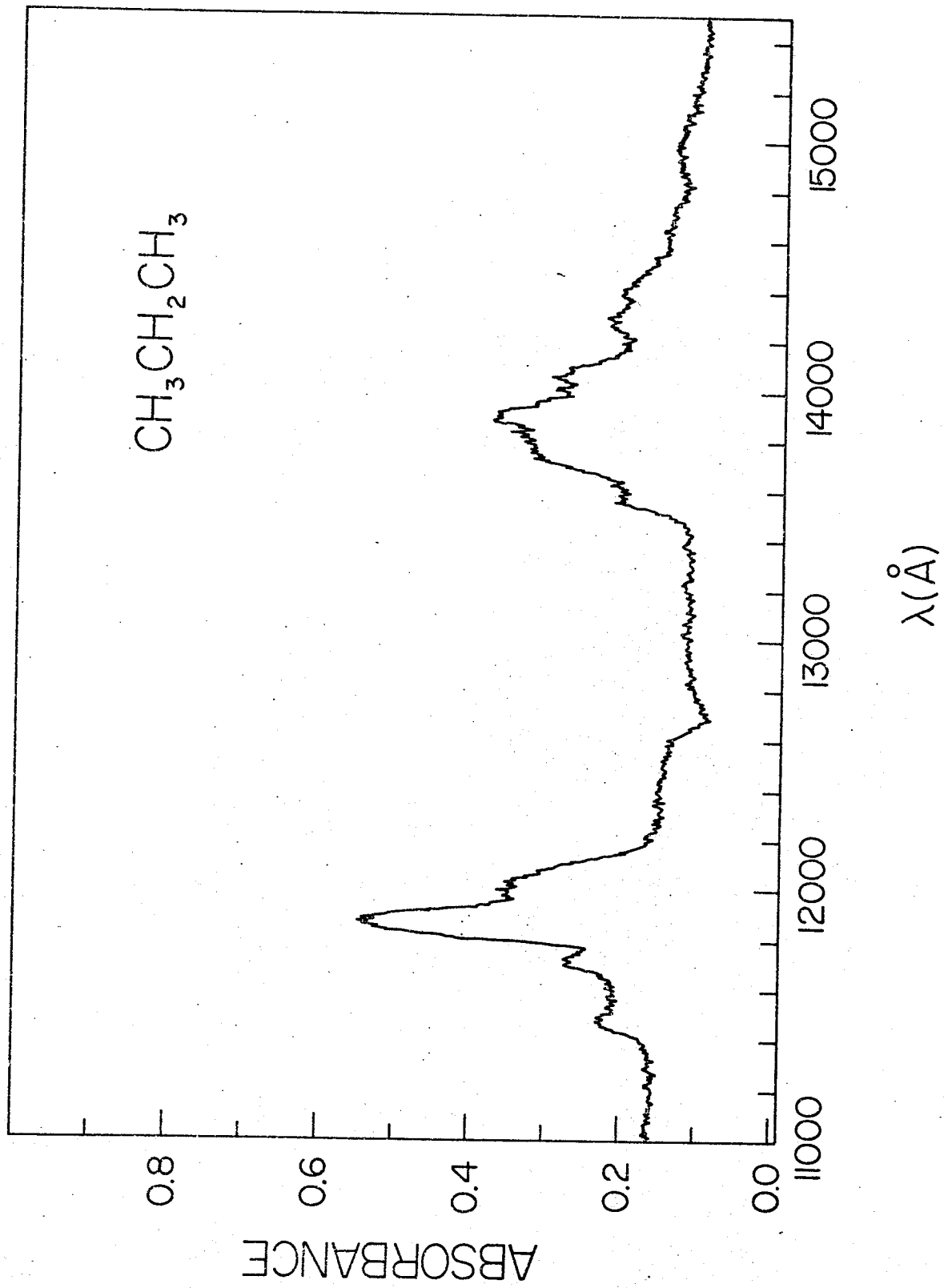
$CH_3CH_2CH_3$
ABSORBANCE
0.0
0.2
0.4
0.6
0.8
11000
12000
13000
14000
15000
λ(Å)

Fig. 2 The overtone spectrum of gas phase (∿30 psi) n-butane at room temperature in the region of $\Delta v_{CH} = 3$. 2.25 m pathlength.

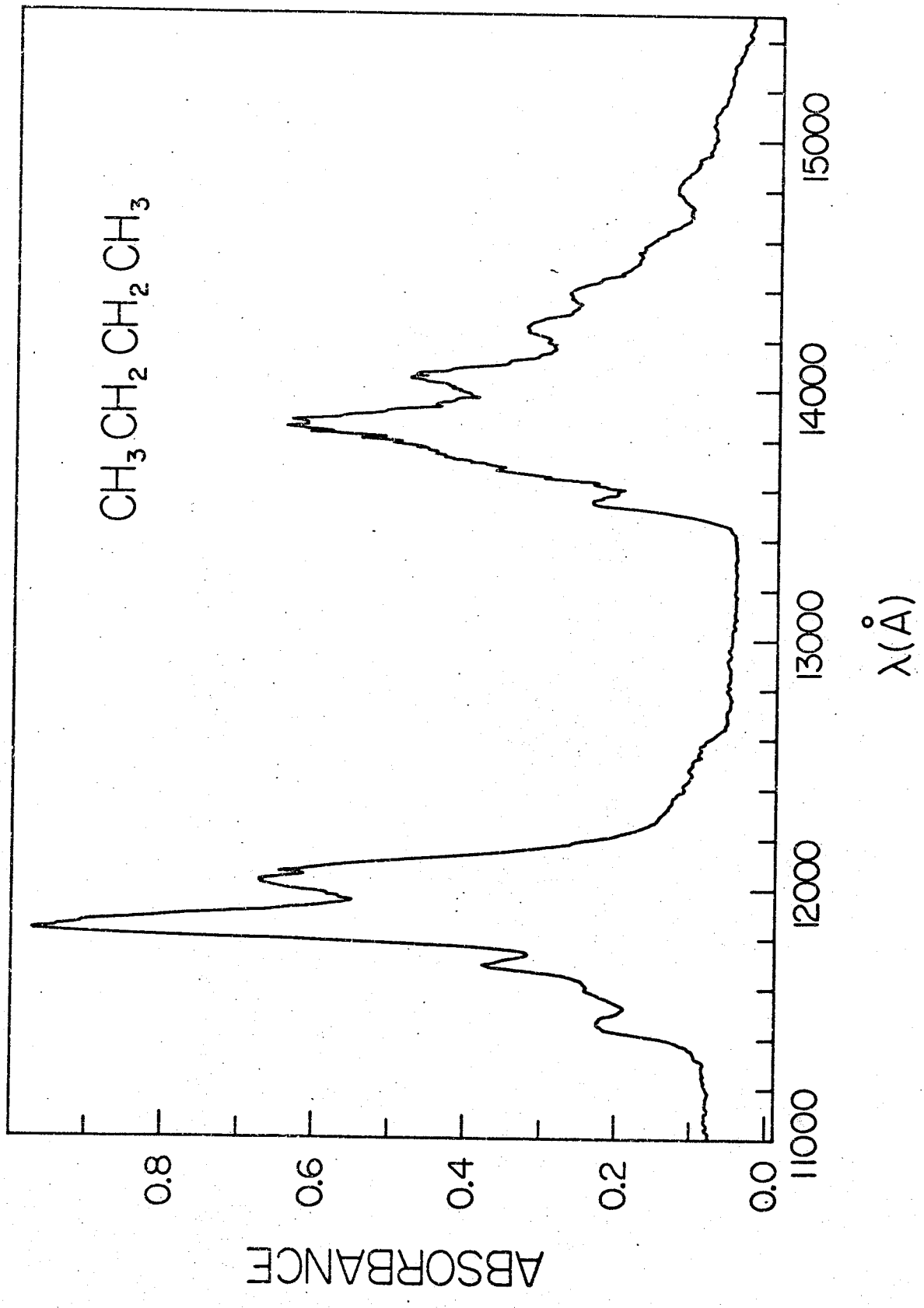
$CH_3CH_2CH_2CH_3$
ABSORBANCE
0.0
0.2
0.4
0.6
0.8
11000
12000
13000
14000
15000
λ(Å)

-17-

Fig. 3 The overtone spectrum of liquid phase n-pentane at room temperature in the region of $\Delta v_{CH} = 3$. 1 cm pathlength.

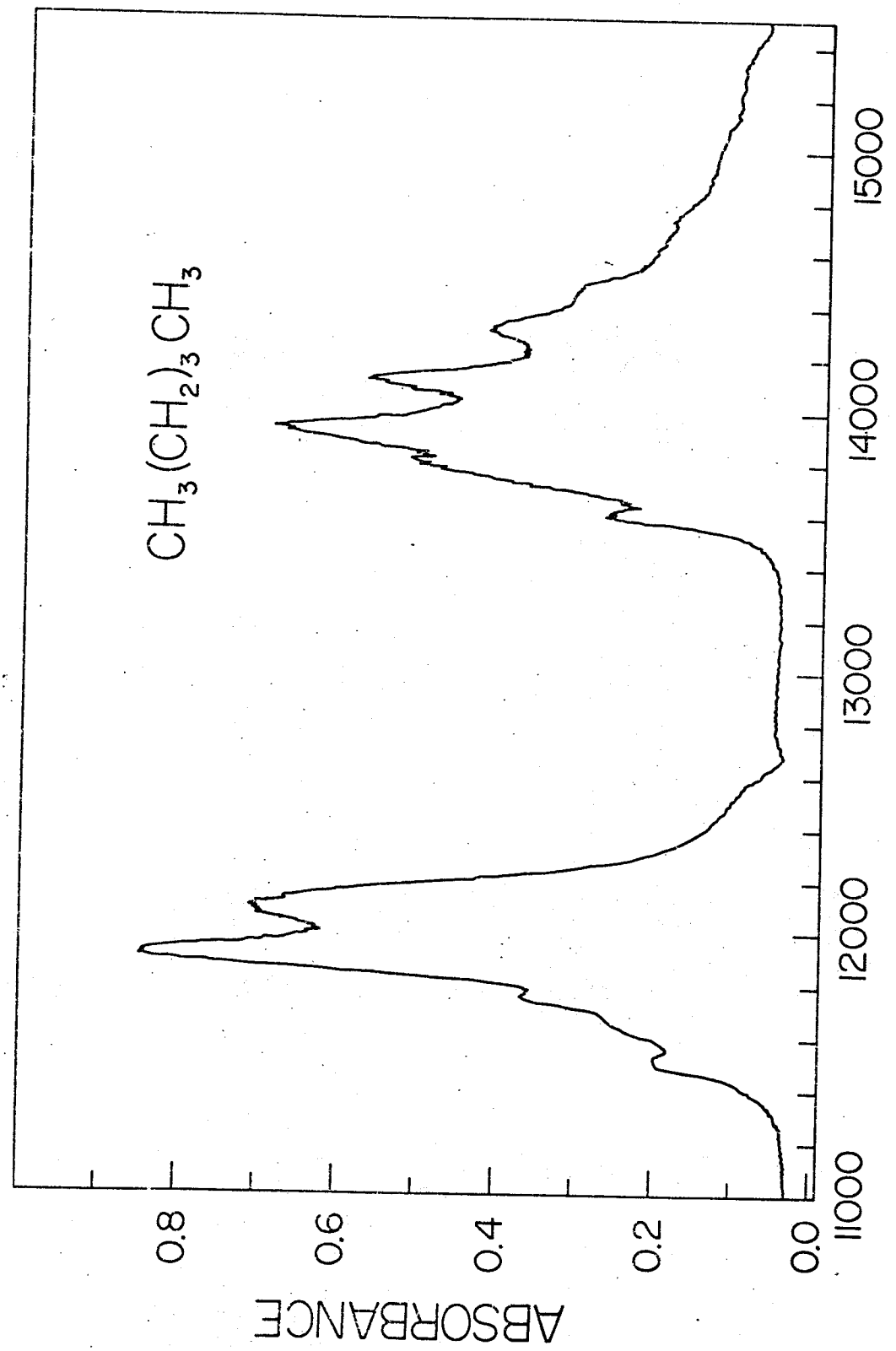
$CH_3(CH_2)_3CH_3$
ABSORBANCE
0.0
0.2
0.4
0.6
0.8
11000
12000
13000
14000
15000
λ(Å)

-18-

Fig. 4 The overtone spectrum of liquid phase n-hexane at room temperature in the region of $\Delta v_{CH} = 3$. 1 cm pathlength.

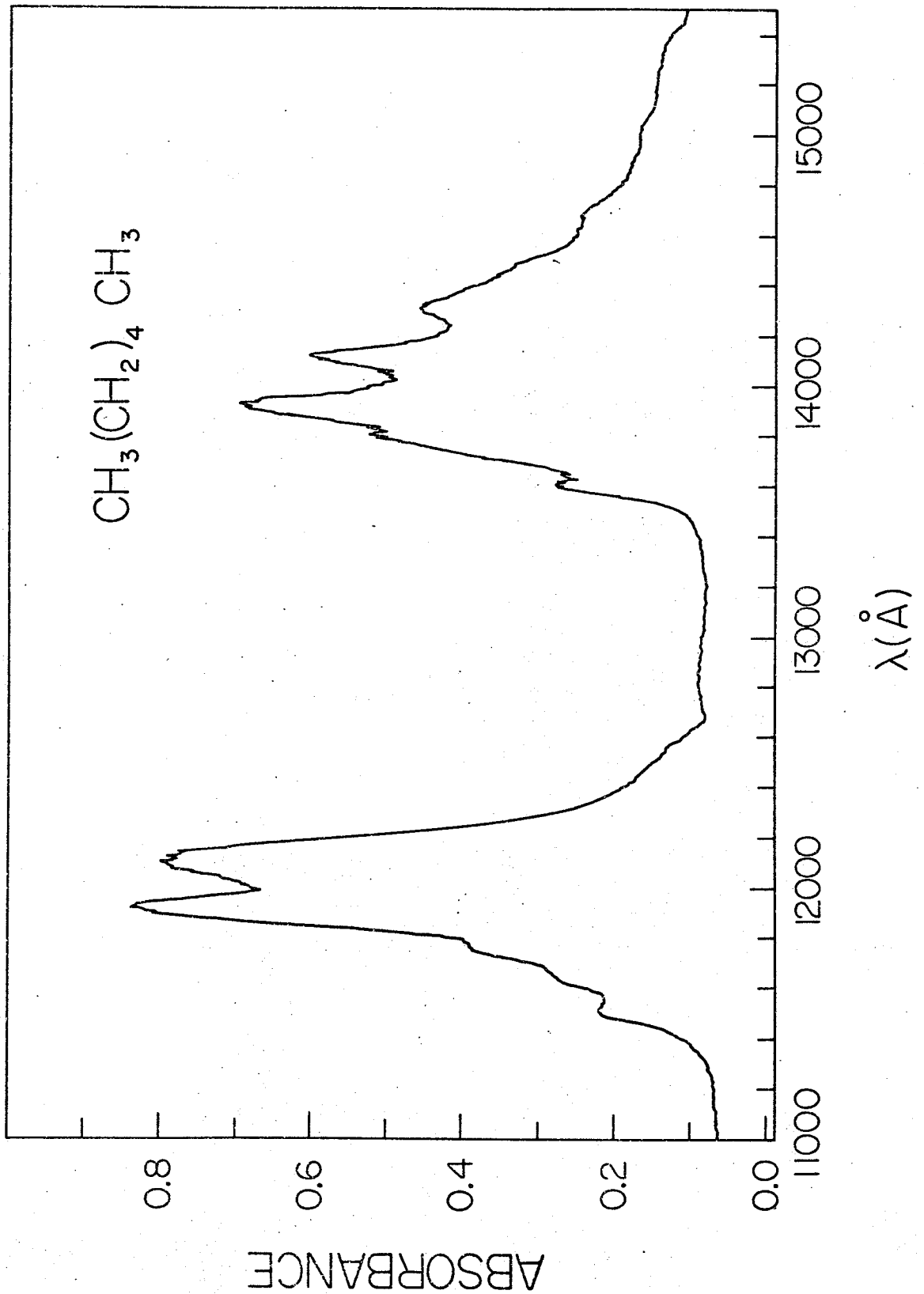
$CH_3(CH_2)_4\ CH_3$
ABSORBANCE
0.0
0.2
0.4
0.6
0.8
11000
12000
13000
14000
15000
λ(Å)

Fig. 5 The overtone spectrum of liquid phase n-heptane at room temperature in the region of $\Delta v_{CH} = 3$. 1 cm pathlength.

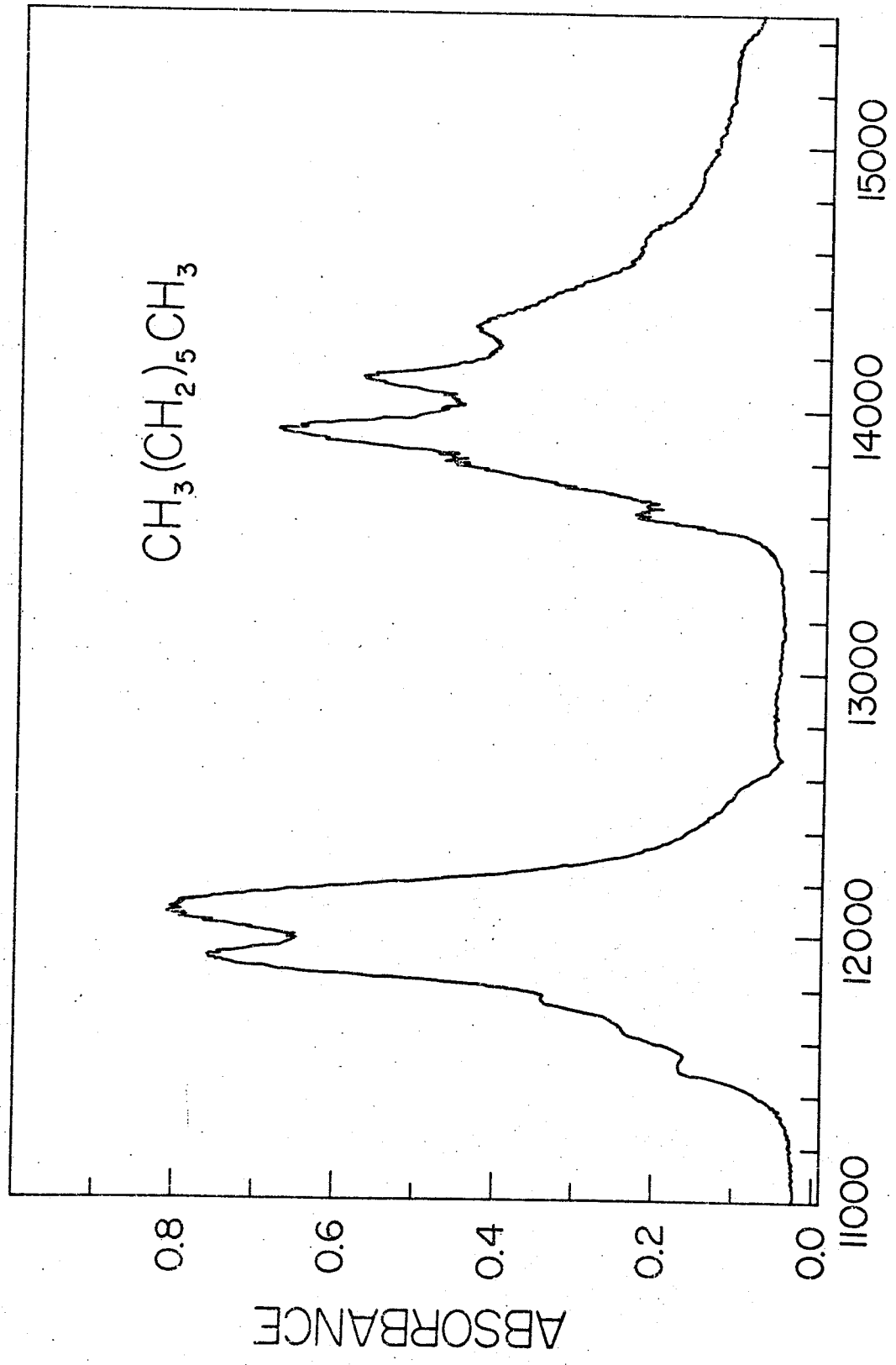
$CH_3(CH_2)_5CH_3$
ABSORBANCE
0.0
0.2
0.4
0.6
0.8
11000
12000
13000
14000
15000
λ(Å)

-20-

Fig. 6 The overtone spectrum of liquid phase 2-methylbutane at room temperature in the region of $\Delta v_{CH} = 3$. 1 cm pathlength.

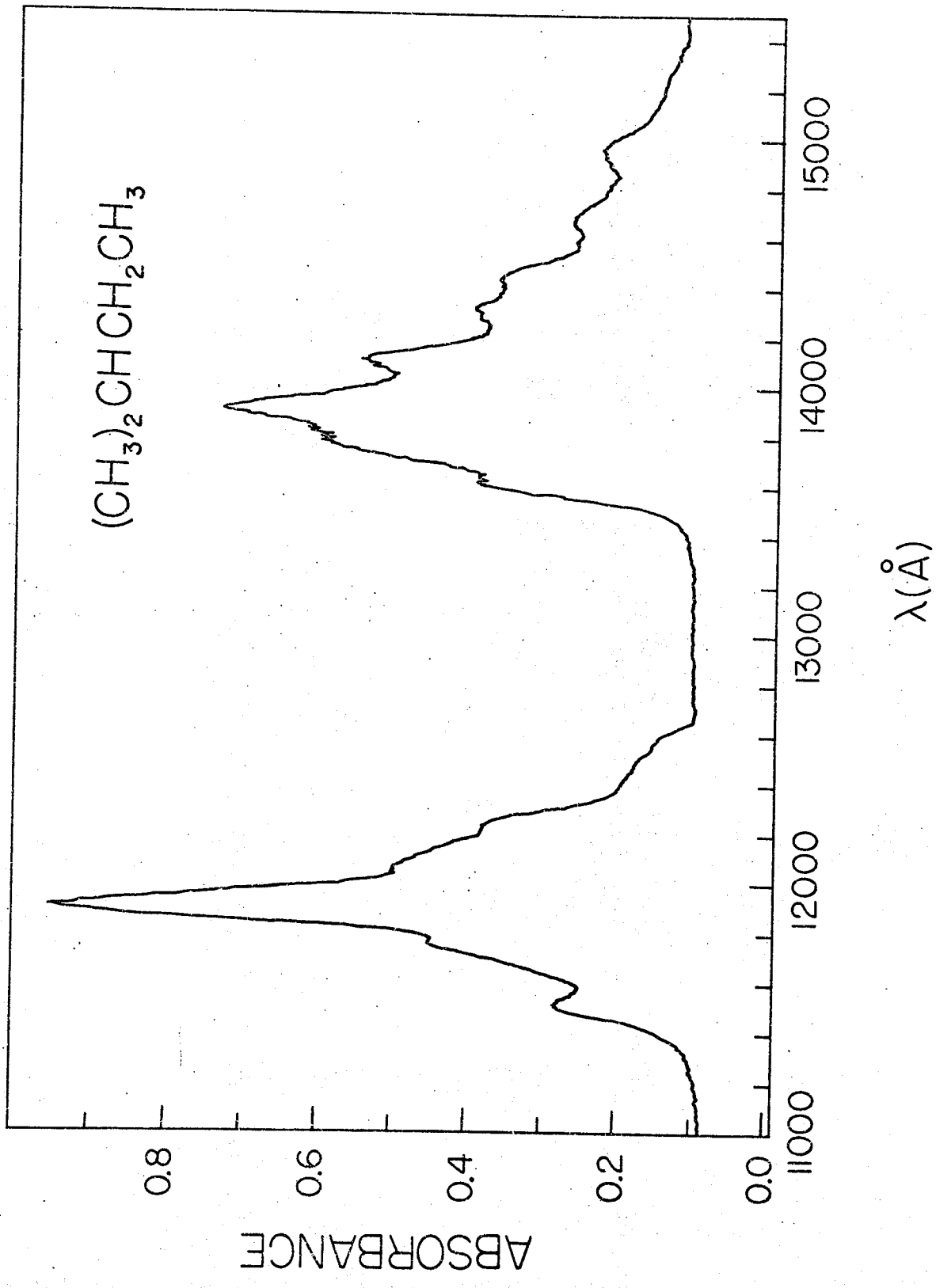
$(CH_3)_2CHCH_2CH_3$
ABSORBANCE
0.0
0.2
0.4
0.6
0.8
11000
12000
13000
14000
15000
λ(Å)

-21-

Fig. 7 The overtone spectrum of liquid phase 3-methylpentane at room temperature in the region of $\Delta v_{CH} = 3$. 1 cm pathlength.

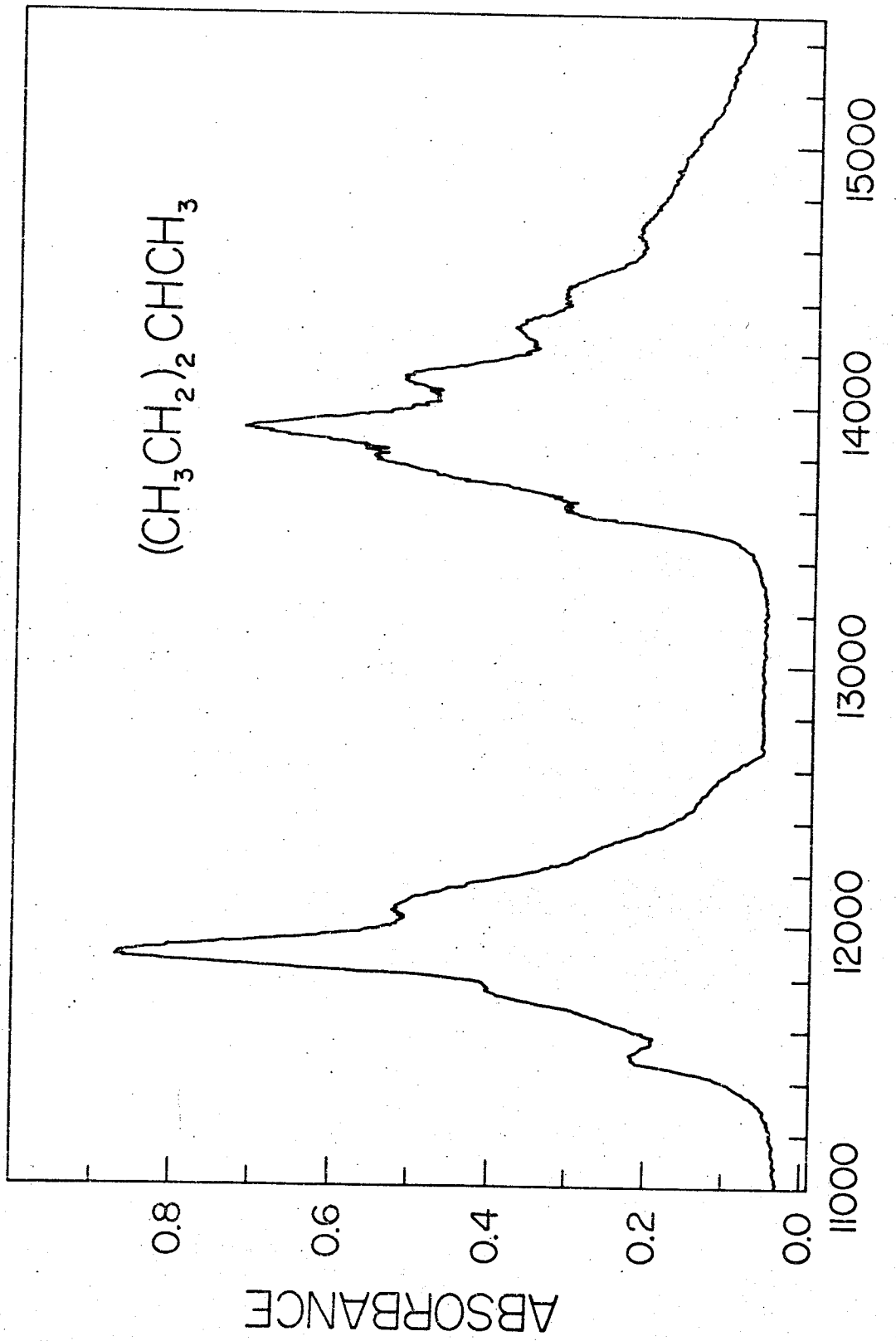
$(CH_3CH_2)_2CHCH_3$
ABSORBANCE
0.0
0.2
0.4
0.6
0.8
11000
12000
13000
14000
15000
λ(Å)

-22-

Fig. 8 The overtone spectrum of liquid phase (under $\sim$ 175 psi) propane at room temperature in the region of $\Delta v_{CH} = 4$. 5 cm pathlength.

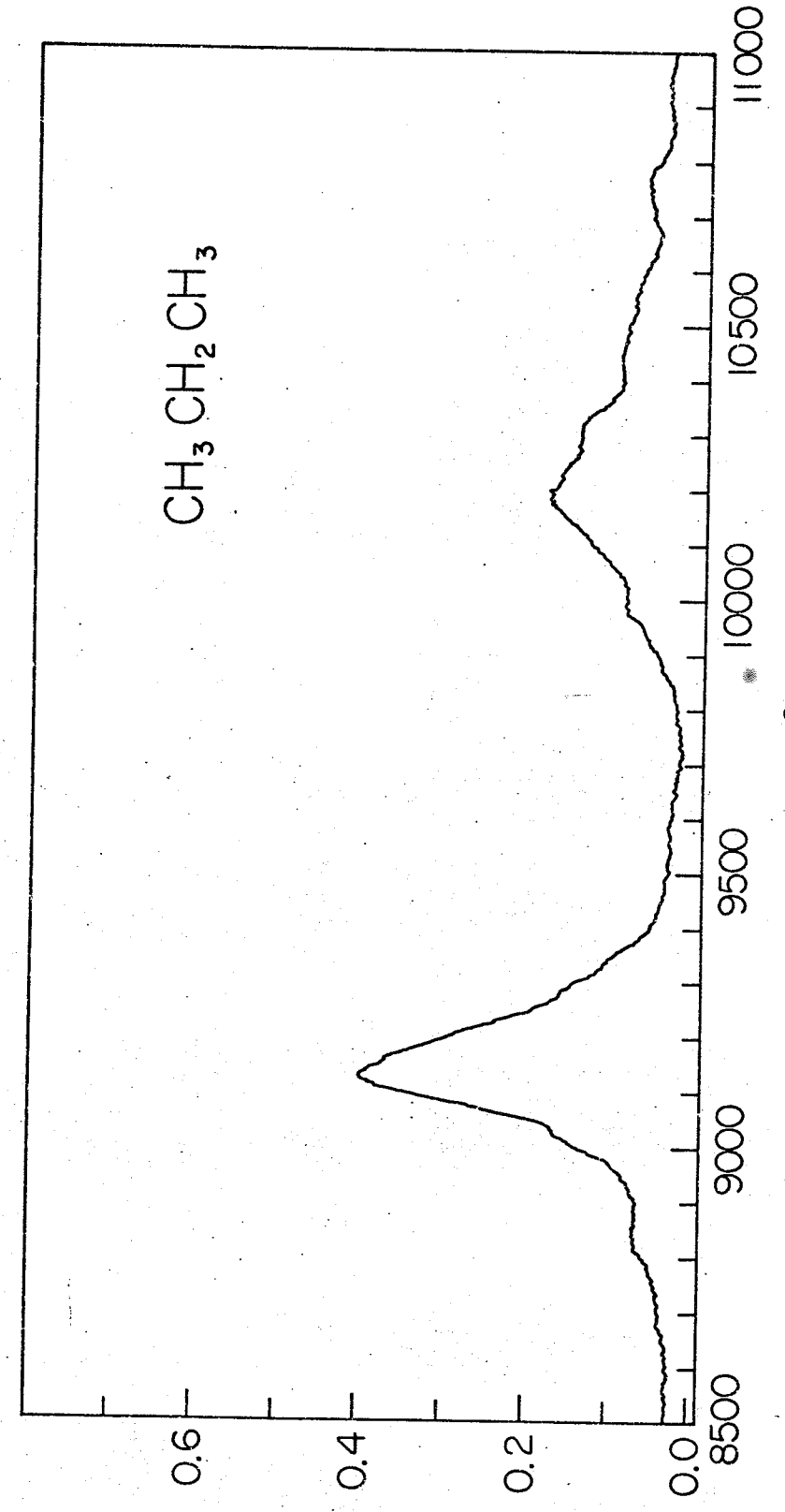
$CH_3\,CH_2\,CH_3$
ABSORBANCE
0.0
0.2
0.4
0.6
8500
9000
9500
10000
10500
11000
λ (Å)

-23-

Fig. 9 The overtone spectrum of liquid phase (under ∿ 60 psi) n-butane at room temperature in the region of $\Delta v_{CH} = 4$. 5 cm pathlength.

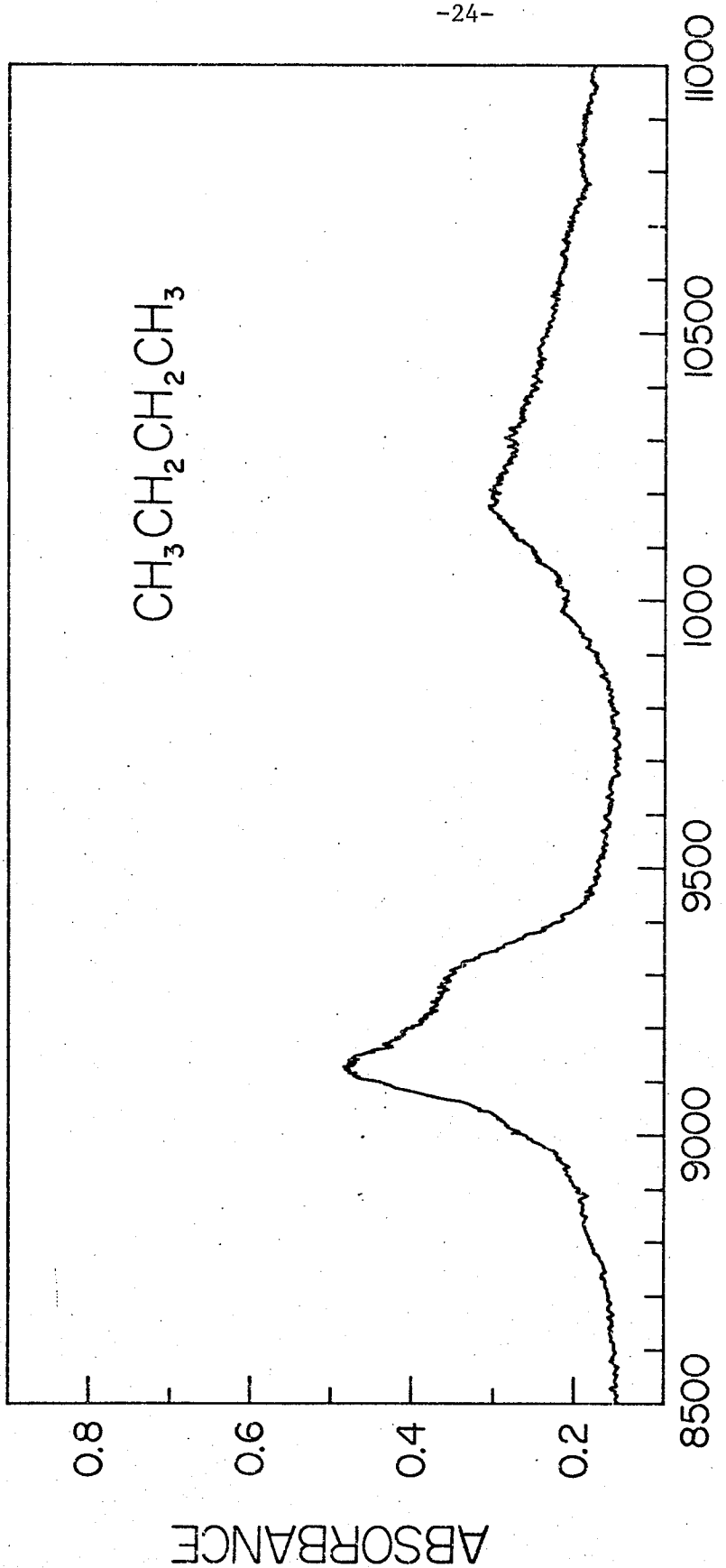
$CH_3CH_2CH_2CH_3$
ABSORBANCE
0.8
0.6
0.4
0.2
8500
9000
9500
1000
10500
11000
λ(Å)

-24-

Fig. 10 The overtone spectrum of liquid phase n-pentane at room temperature in the region of $\Delta v_{CH} = 4$. 10 cm pathlength.

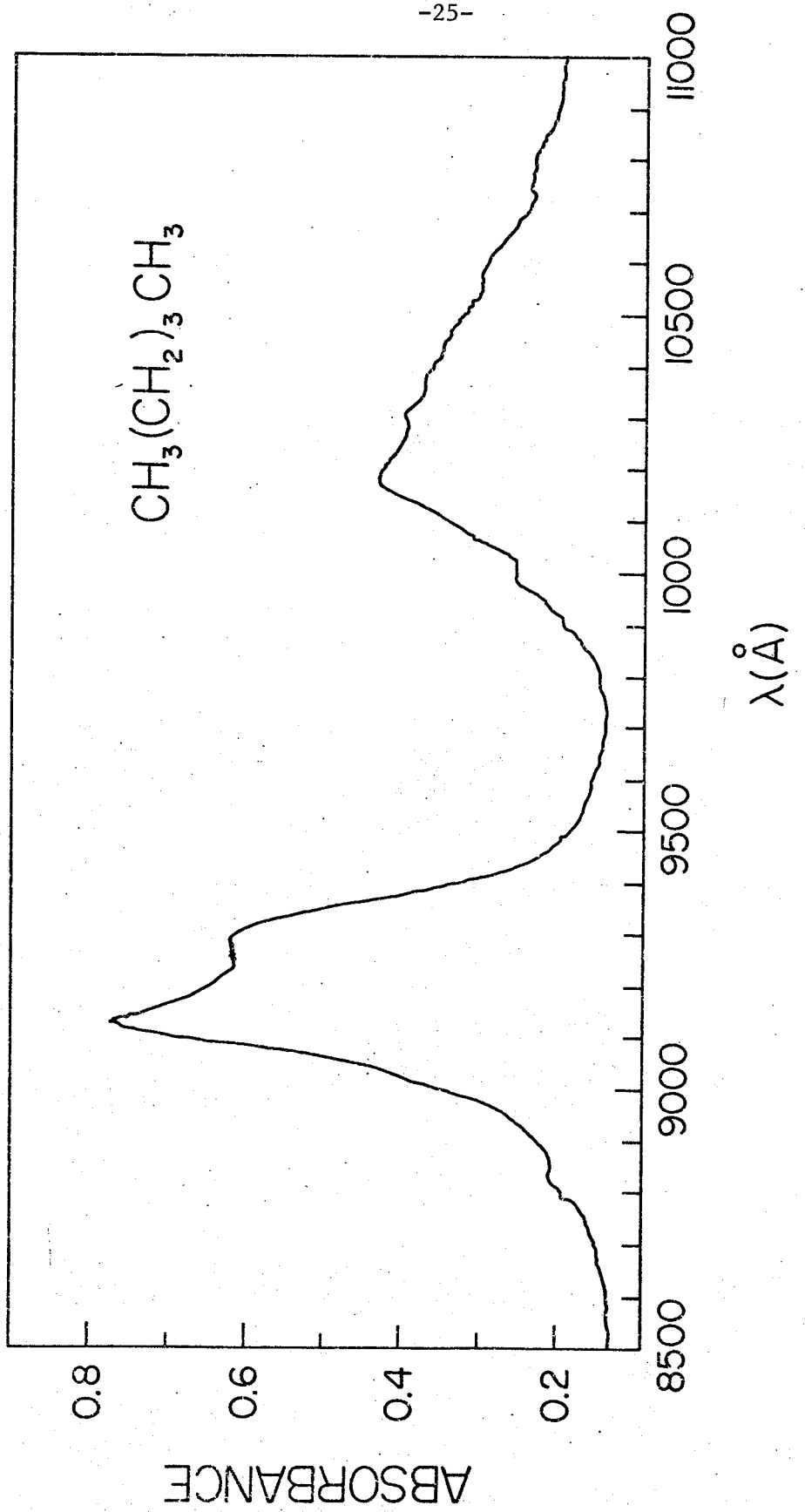
$CH_3(CH_2)_3CH_3$
ABSORBANCE
0.8
0.6
0.4
0.2
8500
9000
9500
1000
10500
11000
λ(Å)

Fig. 11 The overtone spectrum of liquid phase n-hexane at room temperature in the region of $\Delta v_{CH} = 4$. 10 cm path-length.

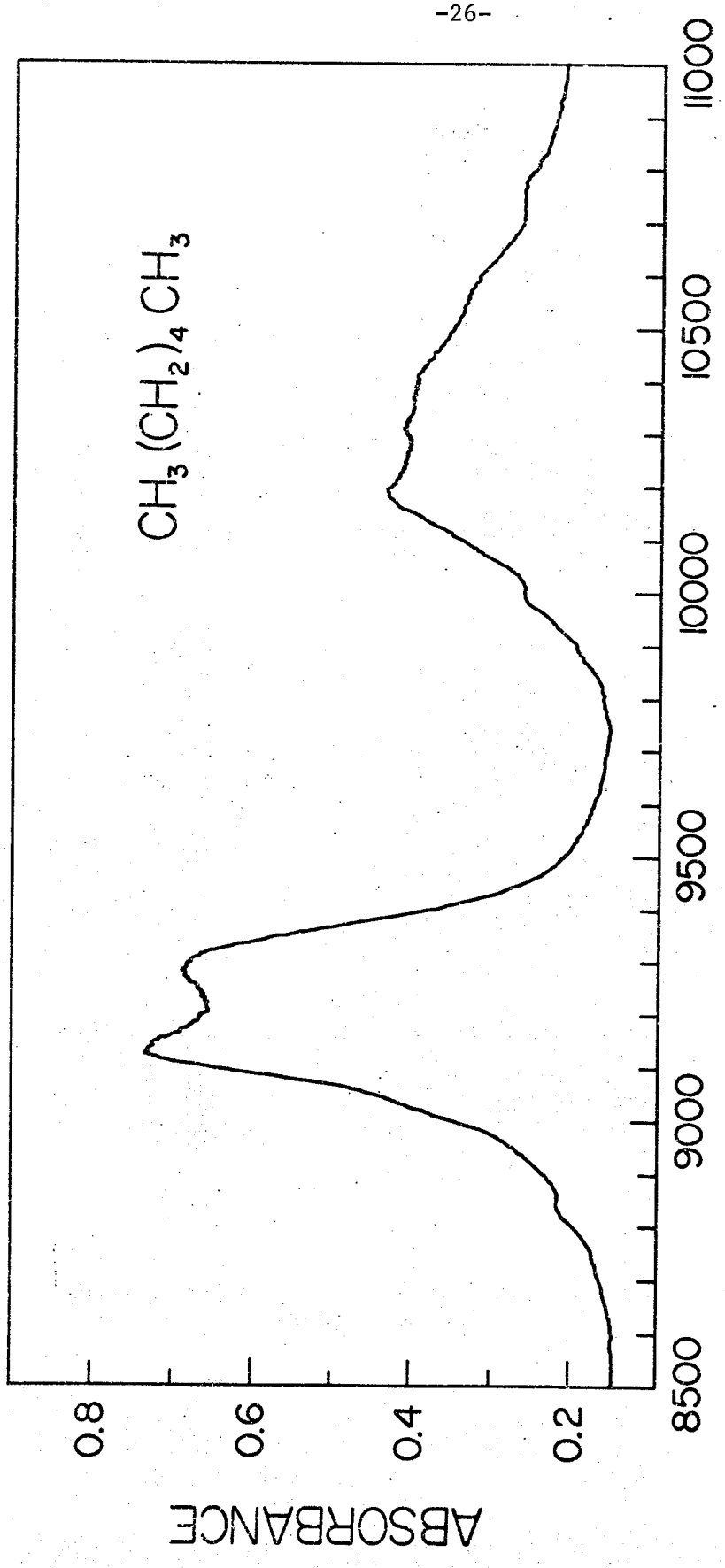
$CH_3(CH_2)_4CH_3$
ABSORBANCE
0.8
0.6
0.4
0.2
8500
9000
9500
10000
10500
11000
λ(Å)

Fig. 12 The overtone spectrum of liquid phase n-heptane at room temperature in the region of $\Delta v_{CH} = 4$. 10 cm path-length.

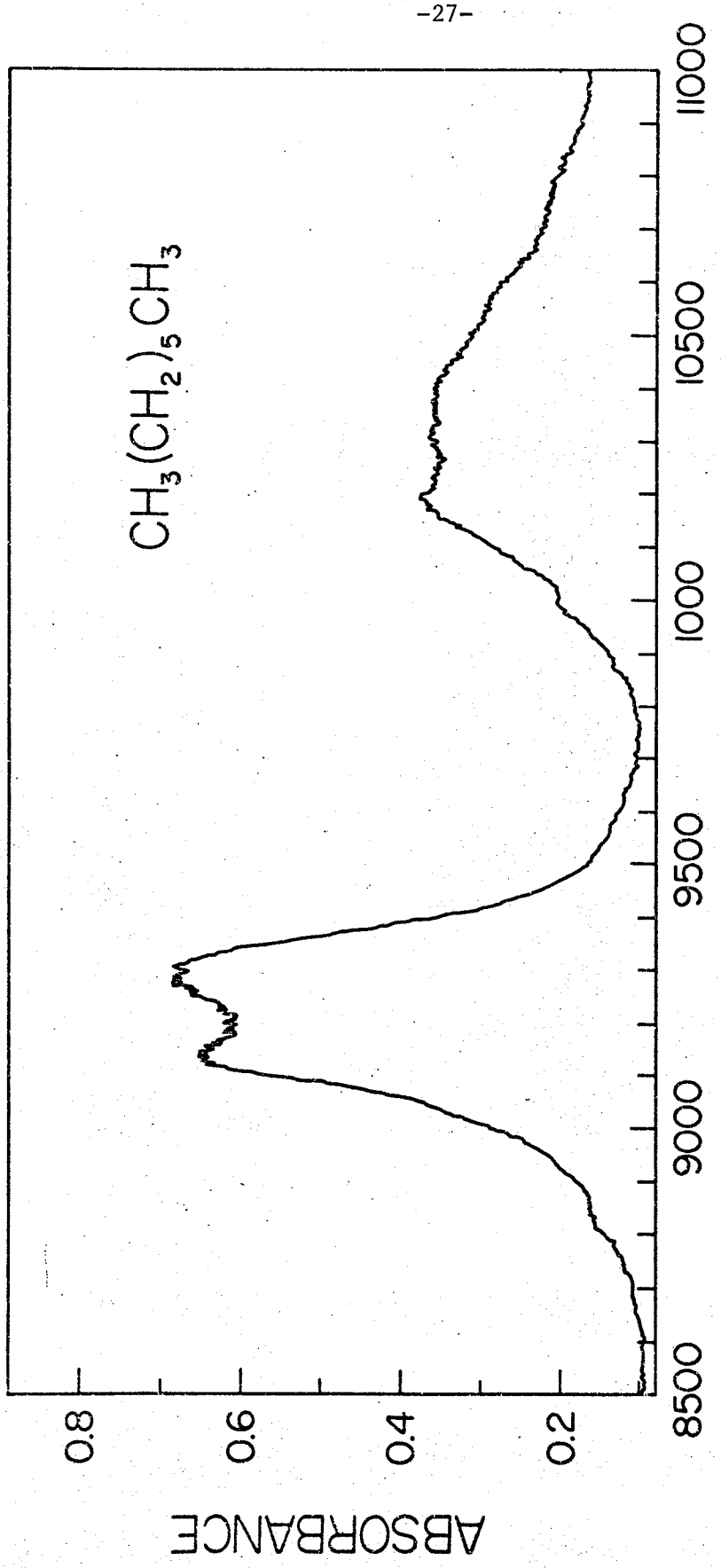
$CH_3(CH_2)_5CH_3$
ABSORBANCE
0.8
0.6
0.4
0.2
8500
9000
9500
1000
10500
11000
λ(Å)

Fig. 13 The overtone spectrum of liquid phase (under ~ 60 psi) isobutane at room temperature in the region of $\Delta v_{CH} = 4$. 5 cm pathlength.

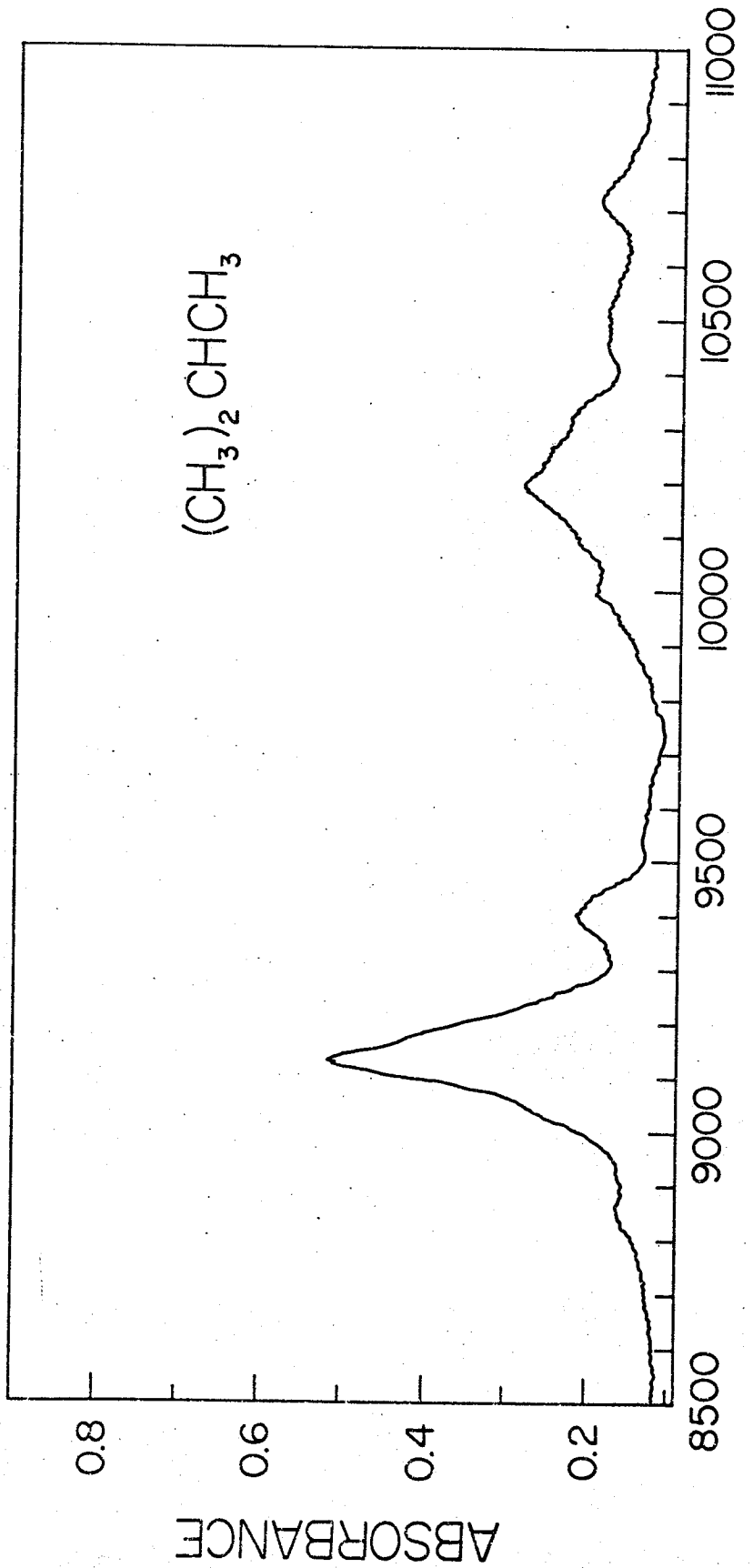
$(CH_3)_2CHCH_3$
ABSORBANCE
0.8
0.6
0.4
0.2
8500
9000
9500
10000
10500
11000
λ(Å)

Fig. 14 The overtone spectrum of liquid phase 2-methylbutane at room temperature in the region of $\Delta v_{CH} = 4$. 10 cm pathlength.

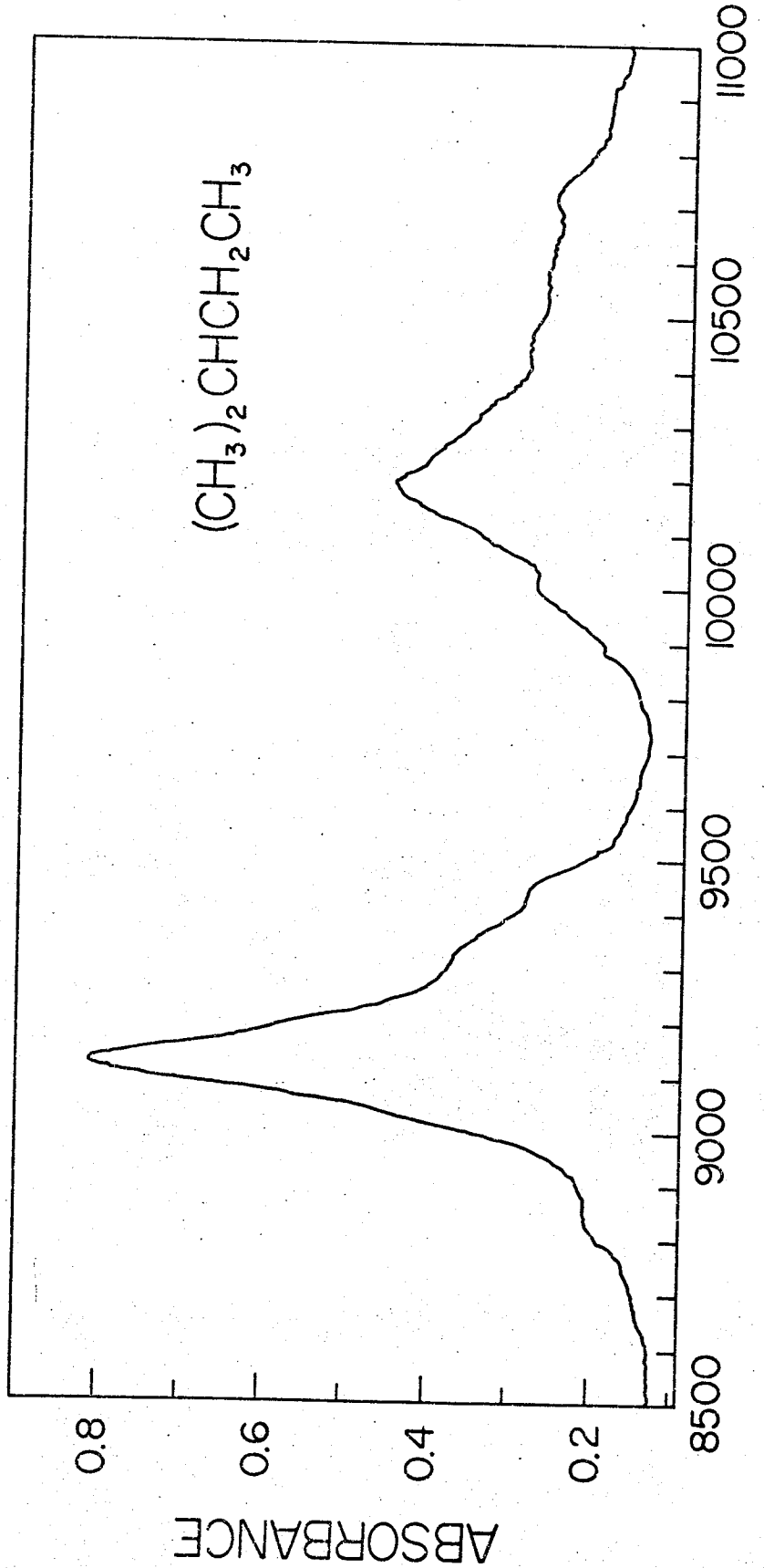
$(CH_3)_2CHCH_2CH_3$
ABSORBANCE
0.8
0.6
0.4
0.2
8500
9000
9500
10000
10500
11000
λ(Å)

Fig. 15 The overtone spectrum of liquid phase 3-methylpentane at room temperature in the region of $\Delta v_{CH} = 4$. 10 cm pathlength.

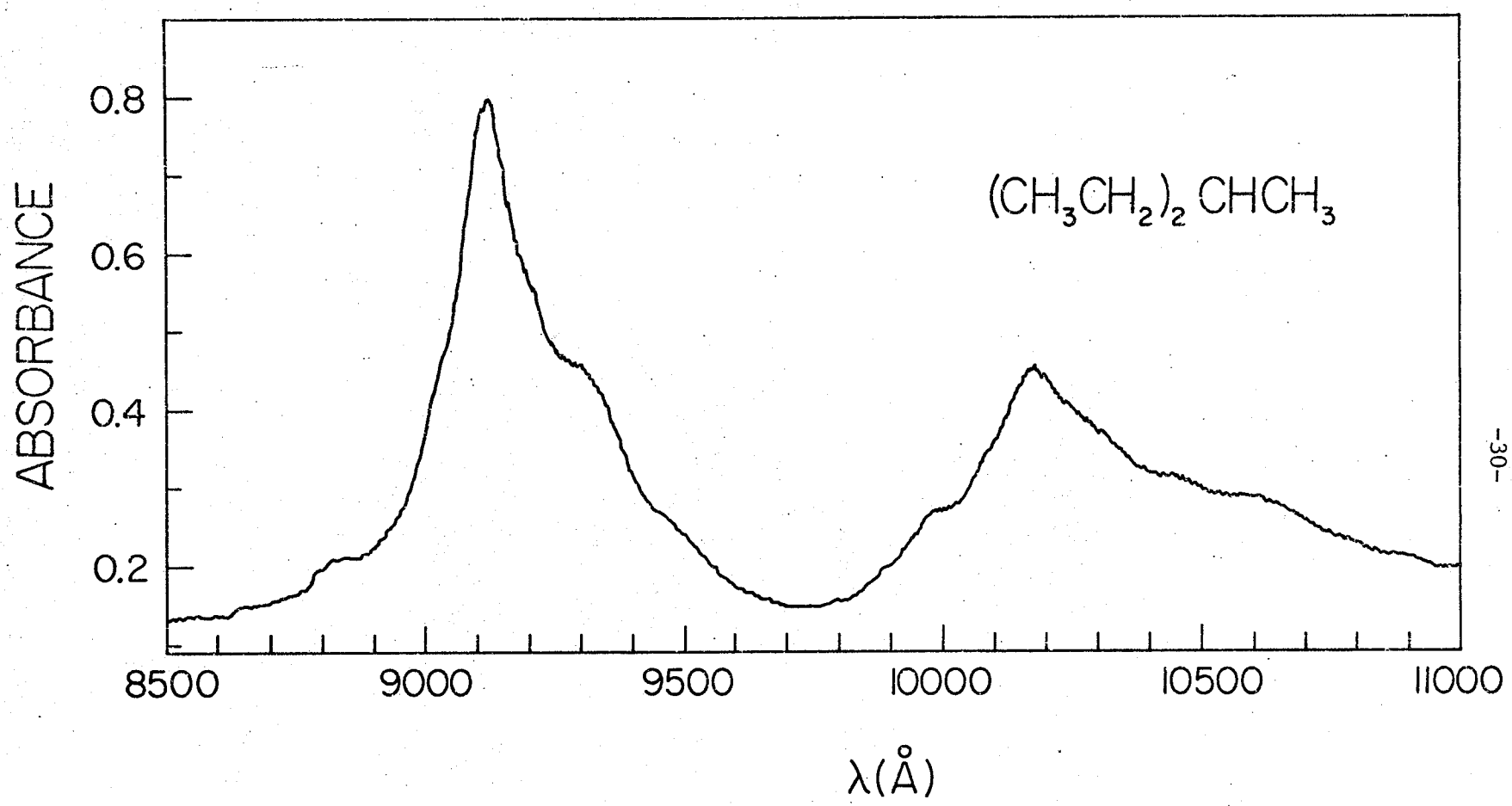
ABSORBANCE
0.8
0.6
0.4
0.2
8500
9000
9500
10000
10500
11000
λ(Å)
(CH3CH2)2 CHCH3

Fig. 16 The overtone spectrum of liquid phase cyclohexane at room temperature in the region of $\Delta v_{CH} = 4$. 10 cm pathlength.

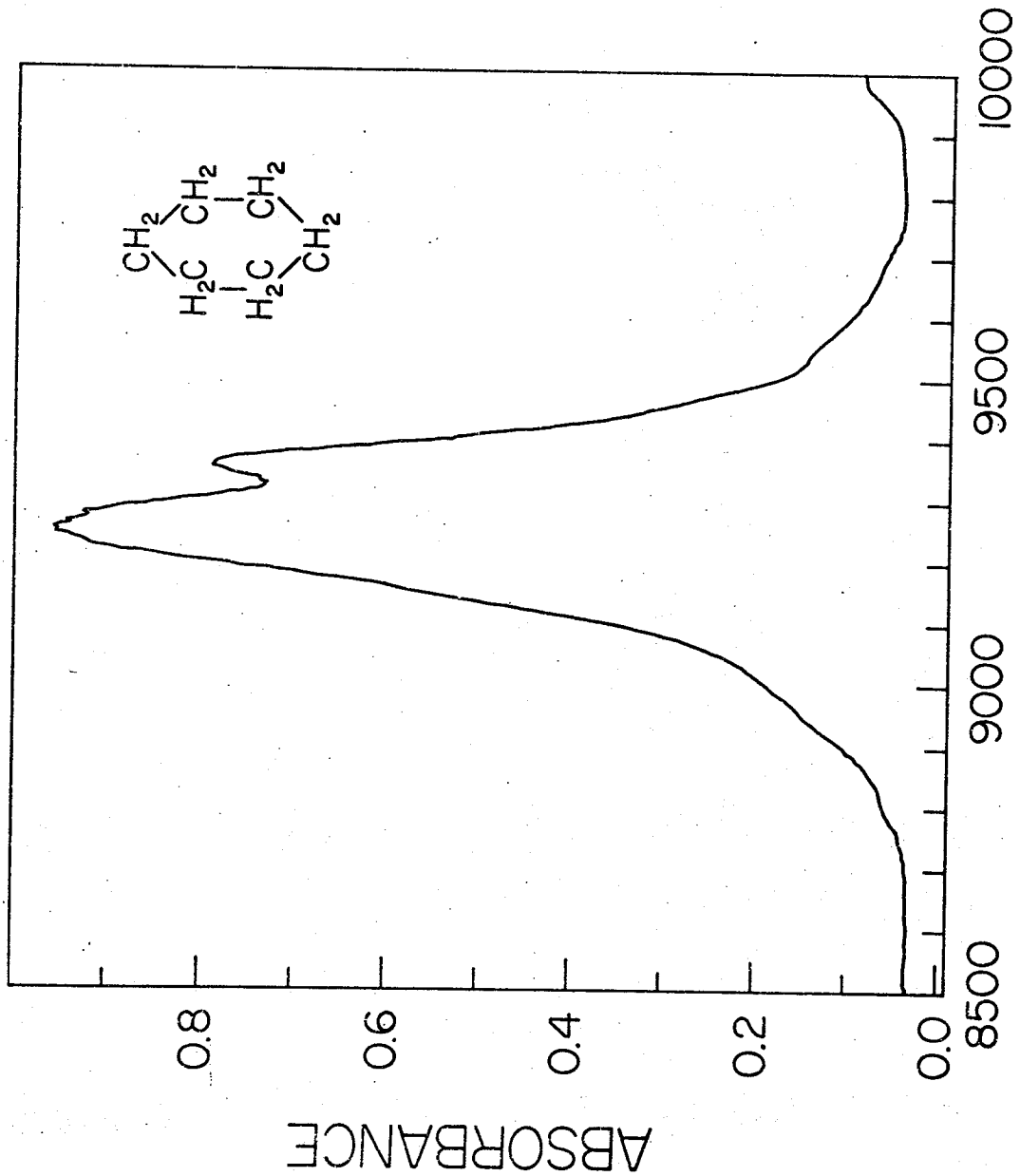
ABSORBANCE
0.0
0.2
0.4
0.6
0.8
8500
9000
9500
10000
λ (Å)
CH2
CH2
CH2
CH2
H2C
H2C

Fig. 17 The overtone spectrum of liquid phase (under $\approx$ 175 psi) propane at room temperature in the region of $\Delta v_{CH} = 5$ and $\Delta v_{CH} = 6$. 5 cm pathlength.

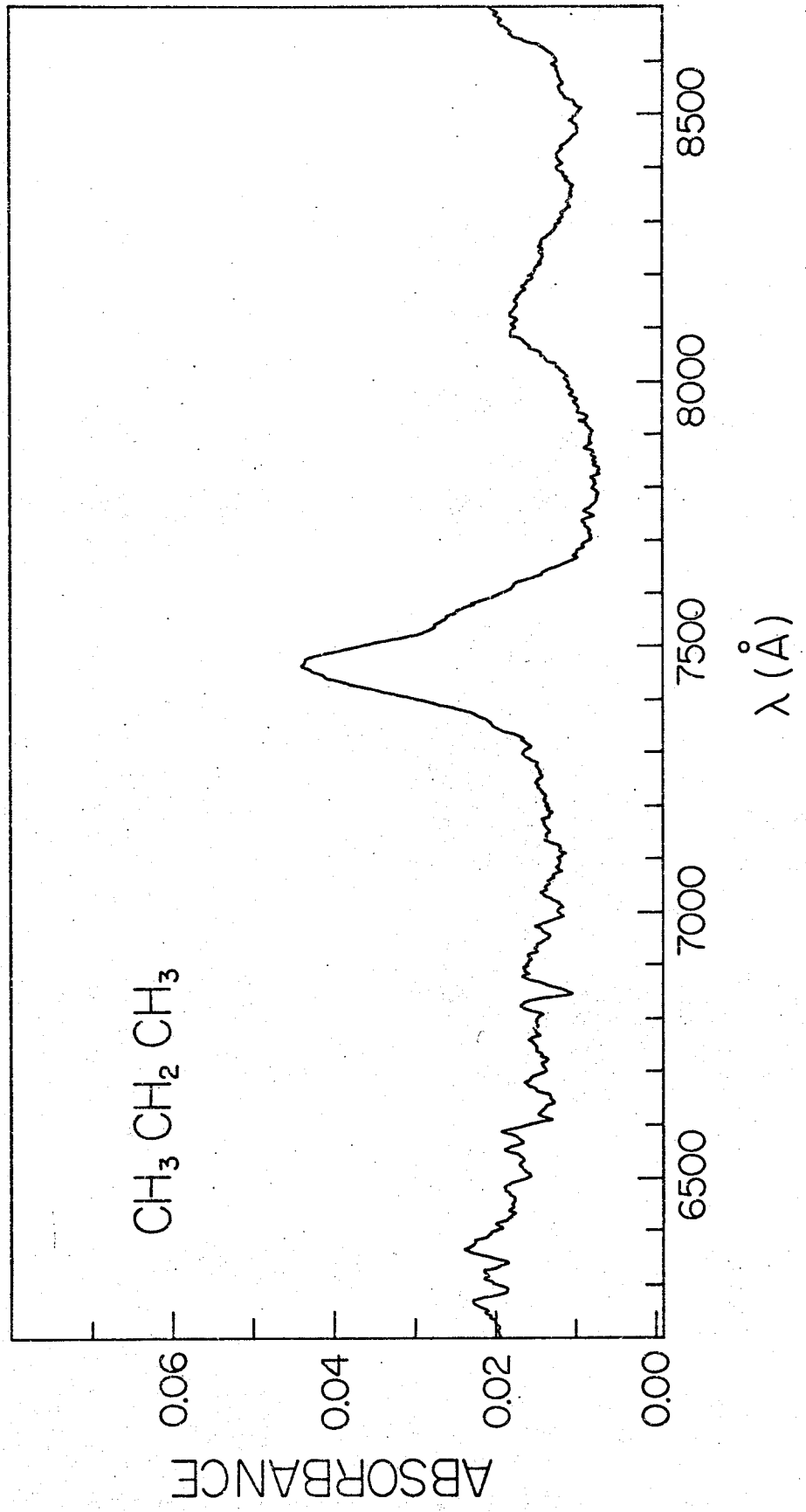
$CH_3\,CH_2\,CH_3$
ABSORBANCE
0.06
0.04
0.02
0.00
6500
7000
7500
8000
8500
λ (Å)

Fig. 18 The overtone spectrum of liquid phase (under $\sim$ 60 psi) n-butane at room temperature in the region of $\Delta v_{CH} = 5$ and $\Delta v_{CH} = 6$. 5 cm pathlength.

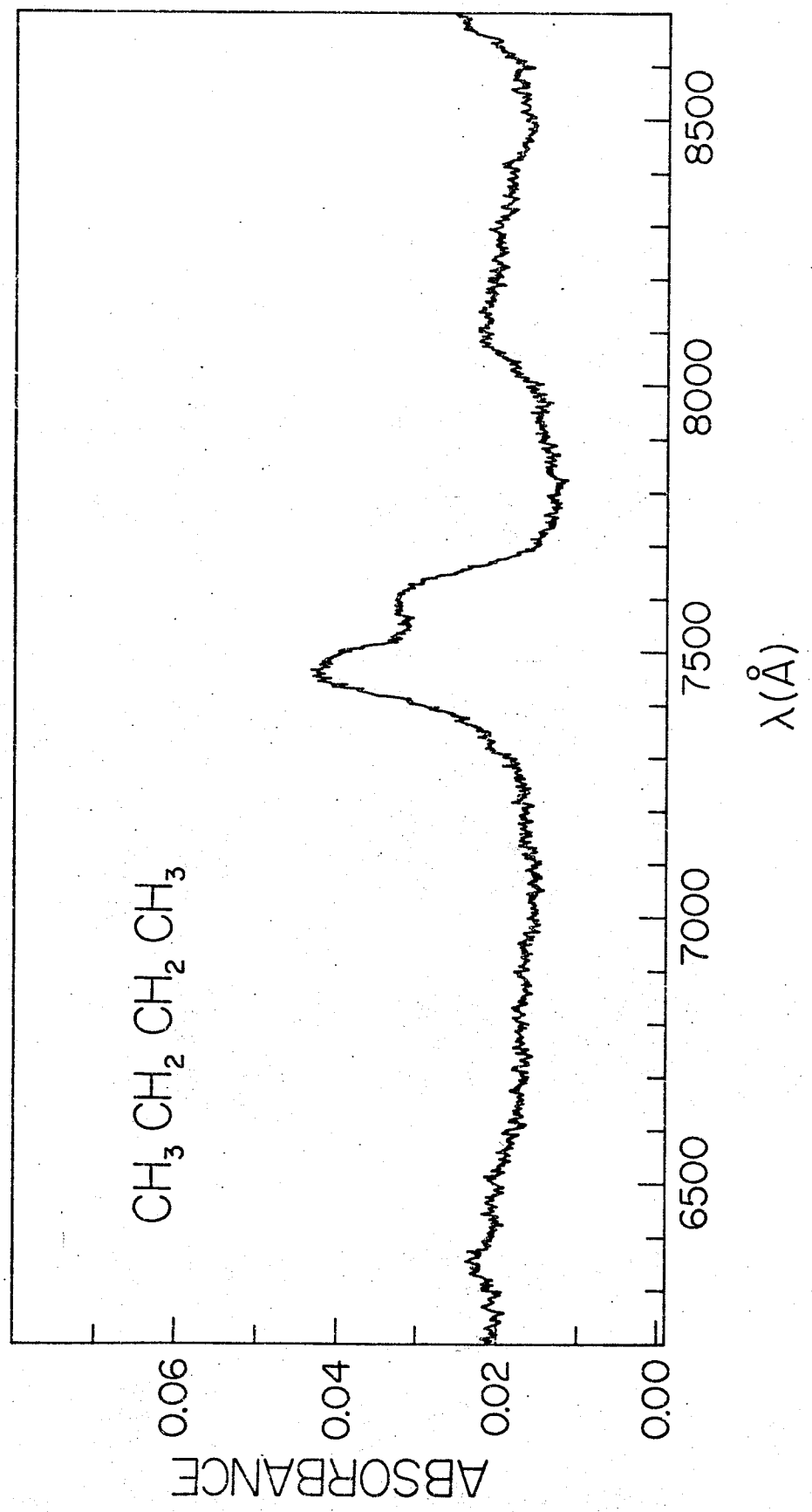
$CH_3\,CH_2\,CH_2\,CH_3$
ABSORBANCE
0.06
0.04
0.02
0.00
6500
7000
7500
8000
8500
λ(Å)

Fig. 19 The overtone spectrum of liquid phase n-pentane at room temperature in the region of $\Delta v_{CH} = 5$ and $\Delta v_{CH} = 6$. 10 cm pathlength.

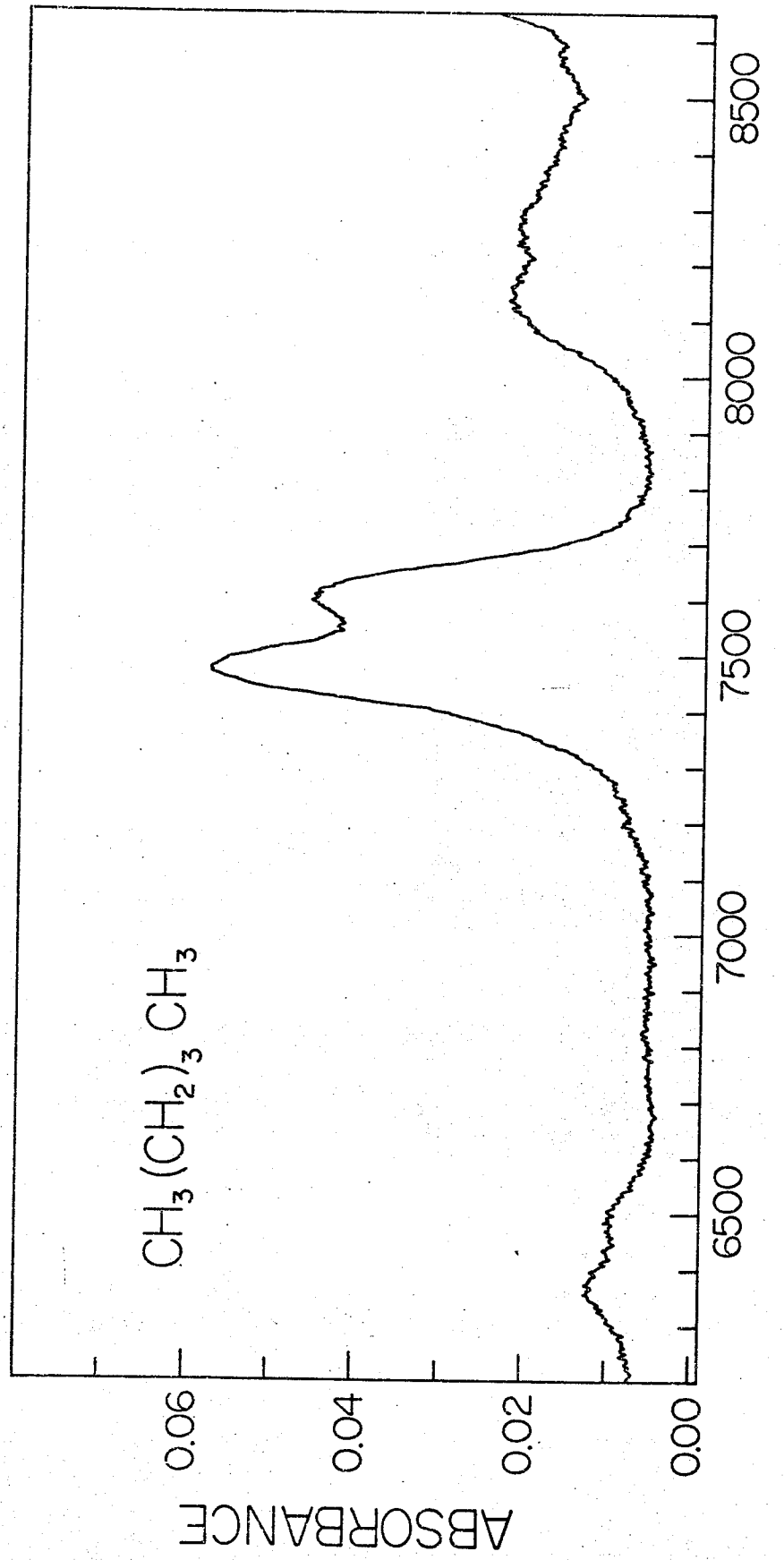
$CH_3(CH_2)_3CH_3$
ABSORBANCE
0.06
0.04
0.02
0.00
6500
7000
7500
8000
8500
λ (Å)

Fig. 20 The overtone spectrum of liquid phase n-hexane at room temperature in the region of $\Delta v_{CH} = 5$ and $\Delta v_{CH} = 6$. 10 cm pathlength.

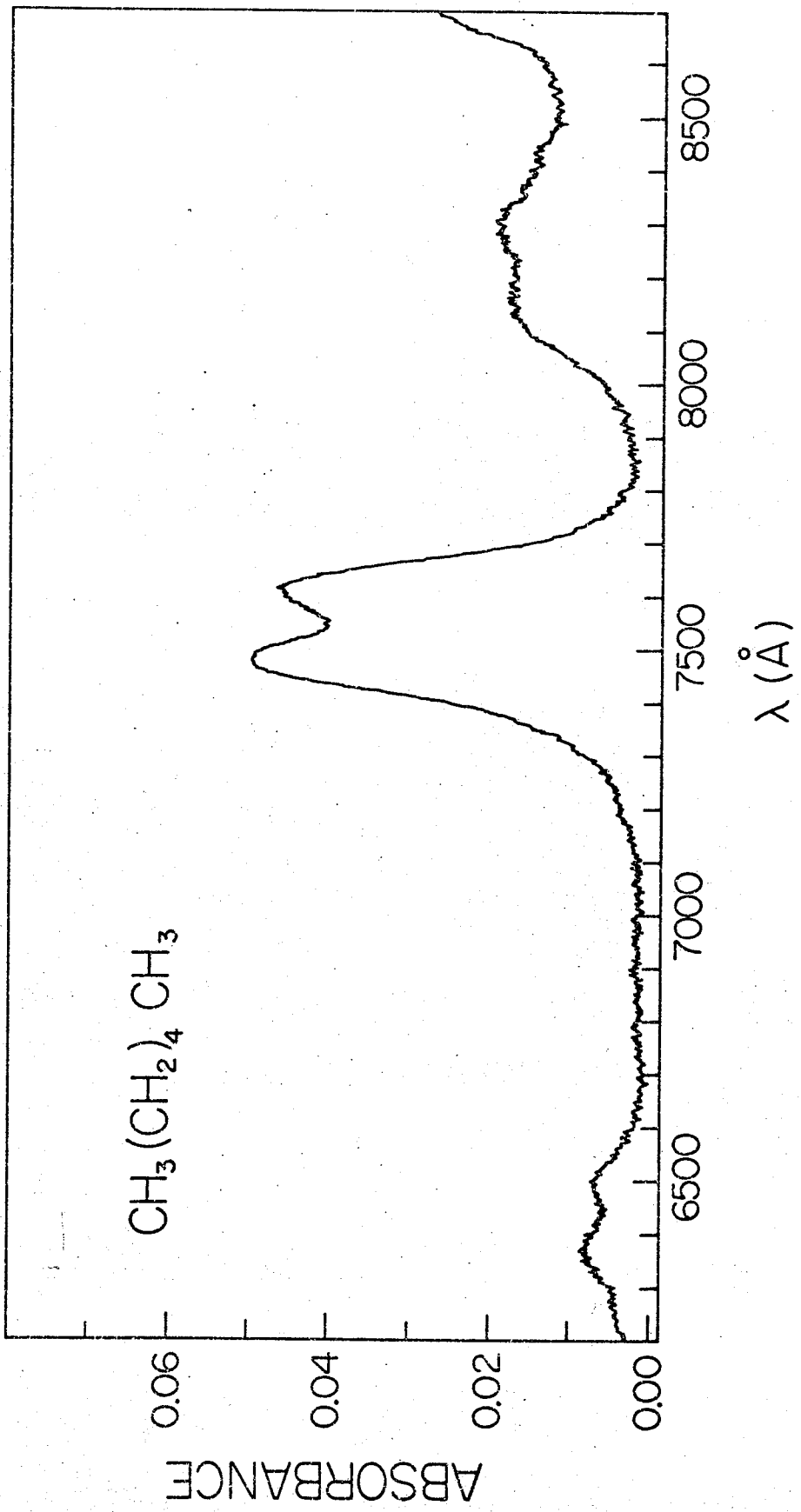
$CH_3(CH_2)_4CH_3$
ABSORBANCE
0.06
0.04
0.02
0.00
6500
7000
7500
8000
8500
λ (Å)

-35-

Fig. 21 The overtone spectrum of liquid phase n-heptane at room temperature in the region of $\Delta v_{CH} = 5$ and $\Delta v_{CH} = 6$. 10 cm pathlength.

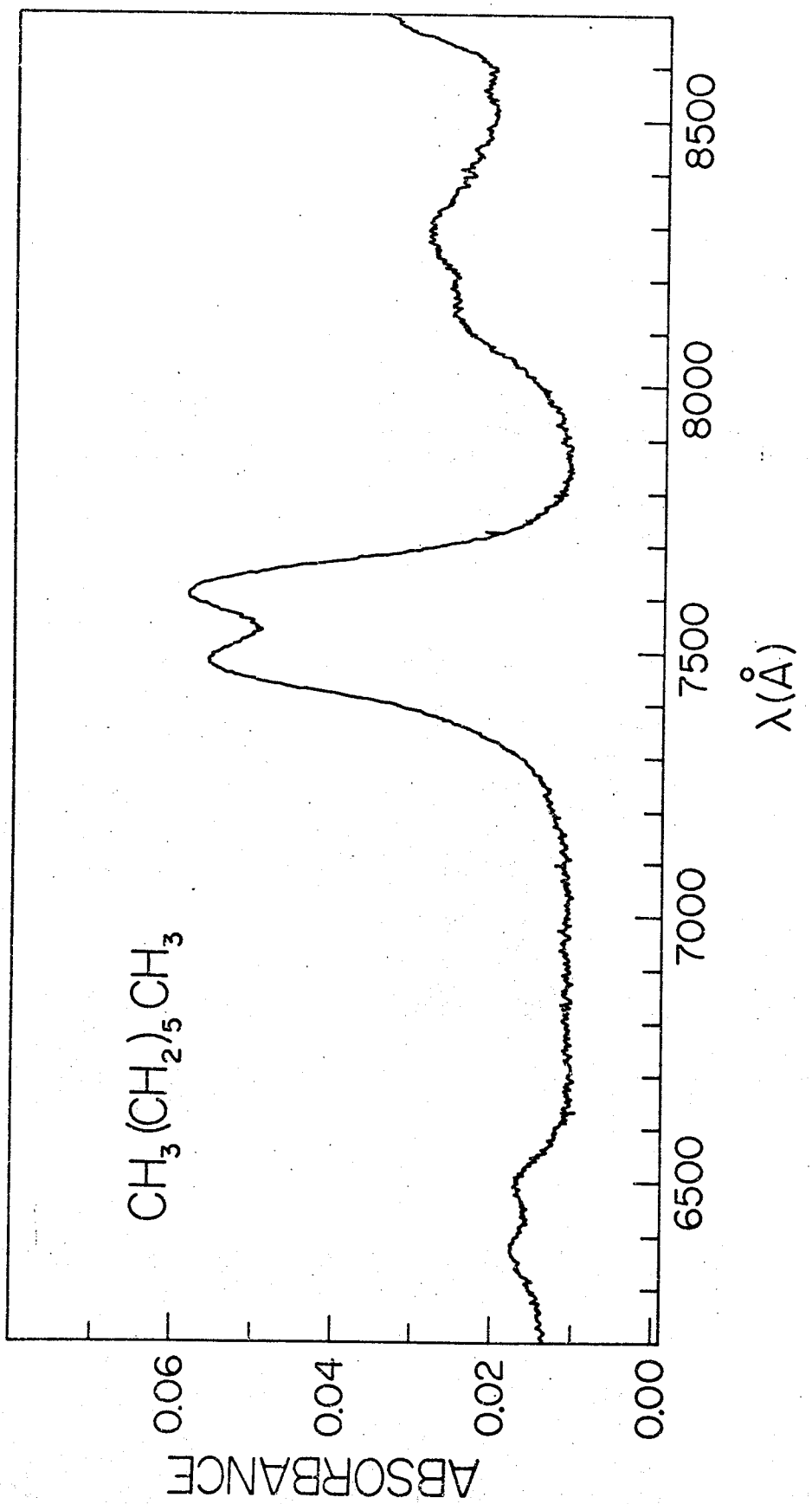
$CH_3(CH_2)_5CH_3$
ABSORBANCE
0.00
0.02
0.04
0.06
6500
7000
7500
8000
8500
λ(Å)

Fig. 22 The overtone spectrum of liquid phase (under ∿ 60 psi) isobutane at room temperature in the region of $\Delta v_{CH} = 5$ and $\Delta v_{CH} = 6$. 5 cm pathlength.

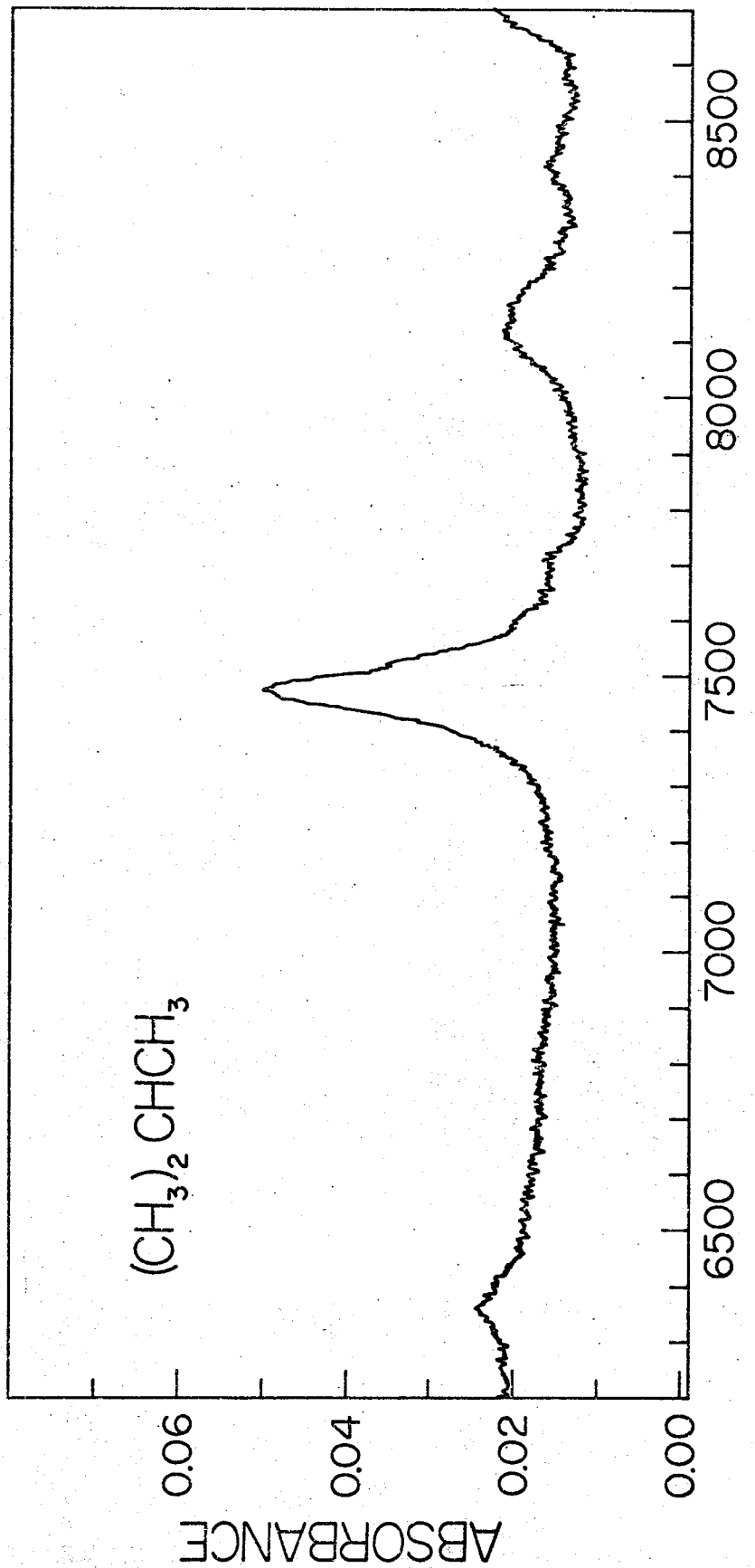
$(CH_3)_2 CHCH_3$
ABSORBANCE
0.00
0.02
0.04
0.06
6500
7000
7500
8000
8500
λ(Å)

-37-

Fig. 23 The overtone spectrum of liquid phase 2-methylbutane at room temperature in the region of $\Delta v_{CH} = 5$ and $\Delta v_{CH} = 6$. 10 cm pathlength.

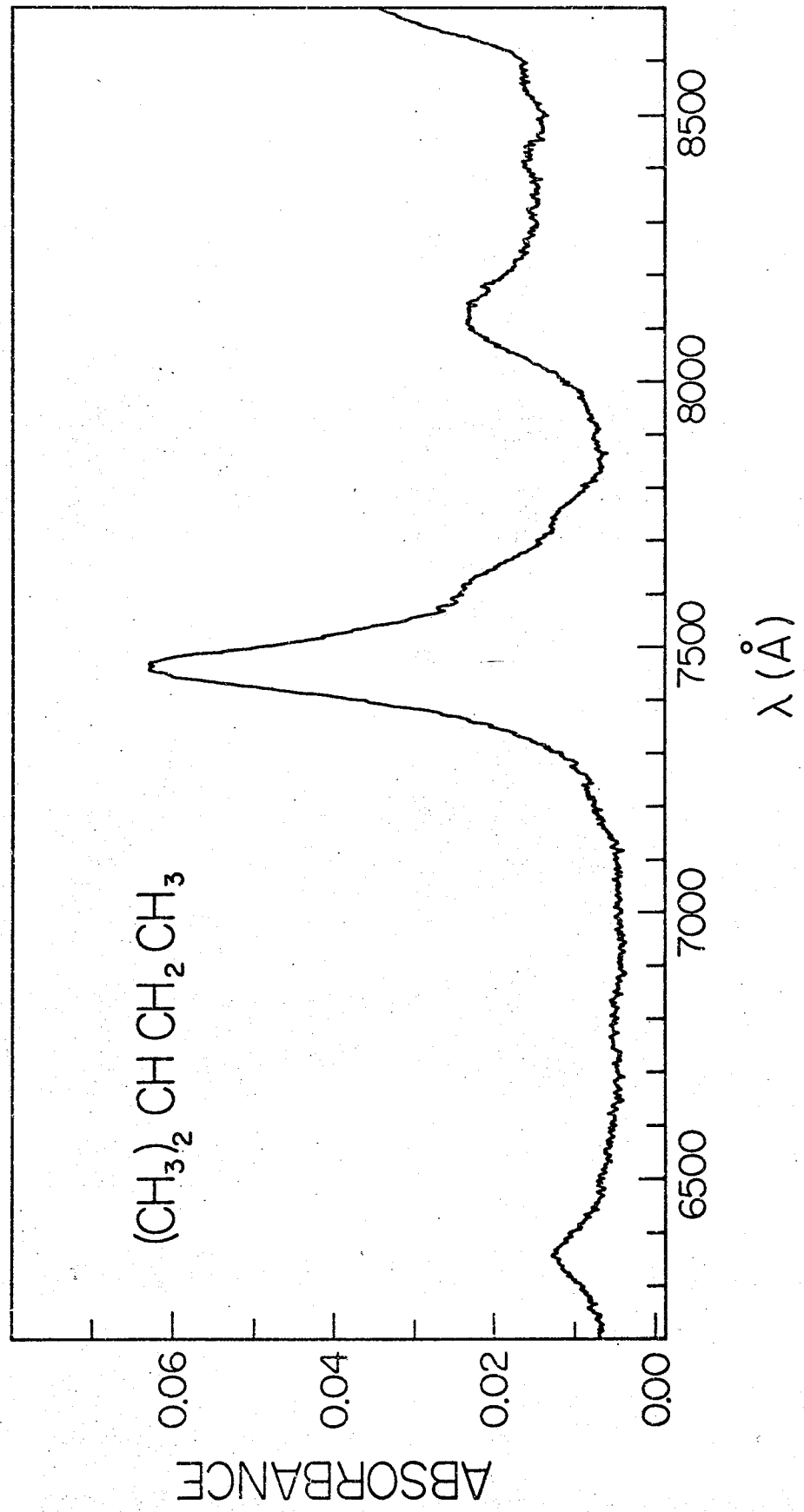
$(CH_3)_2$ CH CH_2 CH_3
ABSORBANCE
0.06
0.04
0.02
0.00
6500
7000
7500
8000
8500
λ (Å)

Fig. 24 The overtone spectrum of liquid phase 3-methylpentane at room temperature in the region of $\Delta v_{CH} = 5$ and $\Delta v_{CH} = 6$. 10 cm pathlength.

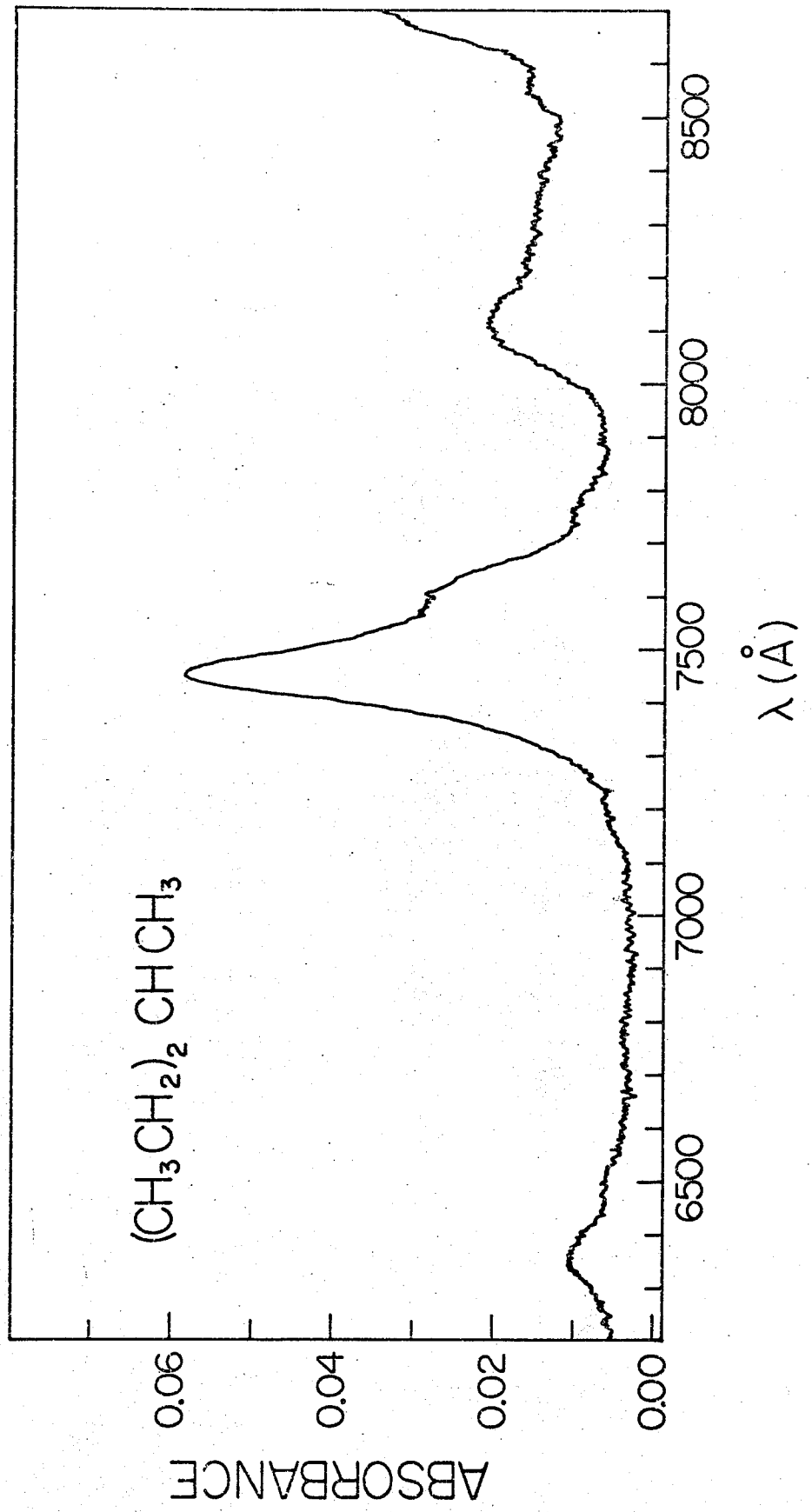
$(CH_3CH_2)_2CHCH_3$
ABSORBANCE
0.00
0.02
0.04
0.06
6500
7000
7500
8000
8500
λ (Å)

Fig. 25 The overtone spectrum of liquid phase cyclohexane at room temperature in the region of $\Delta v_{CH} = 5$ and $\Delta v_{CH} = 6$. 10 cm pathlength.

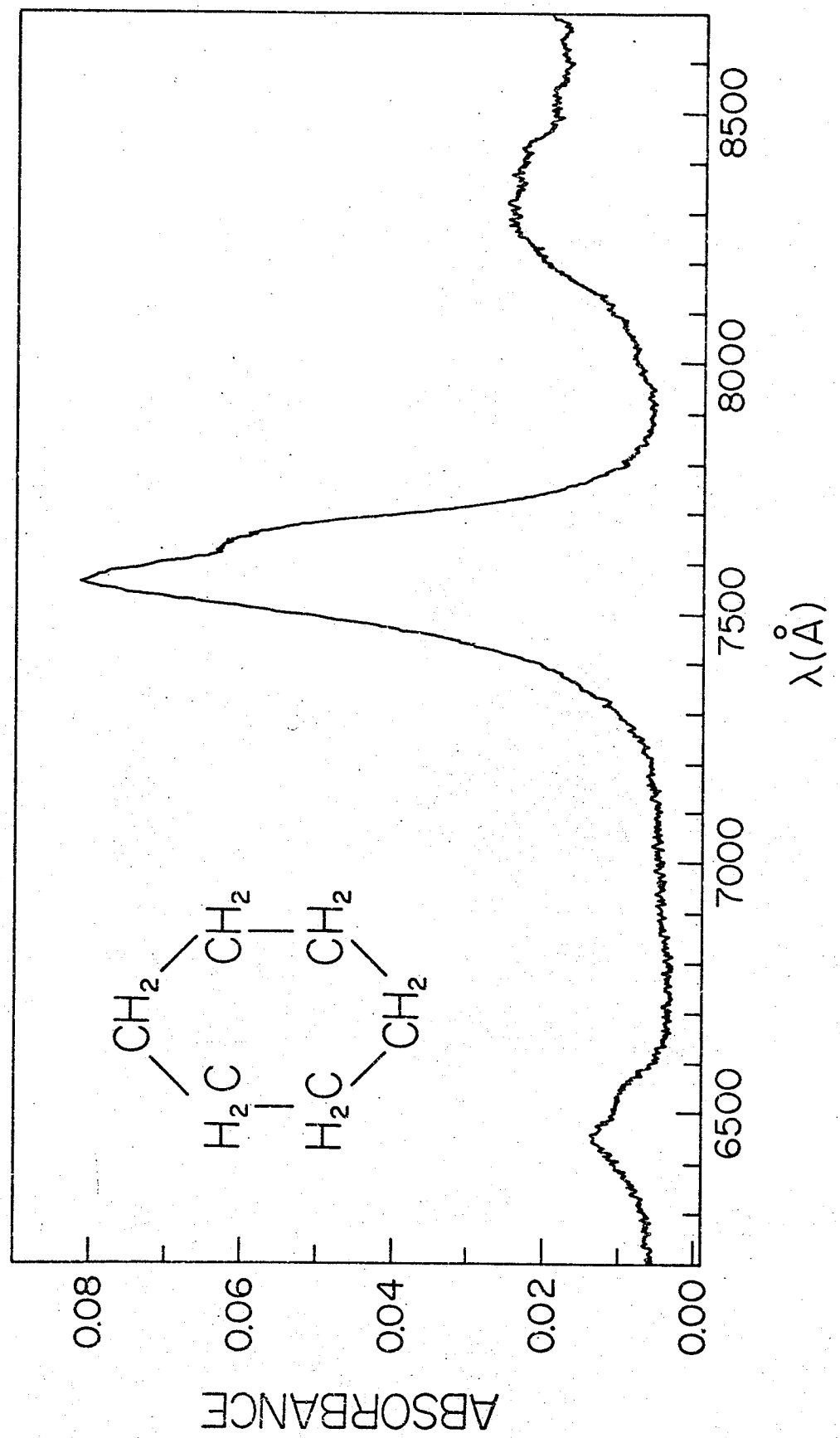
ABSORBANCE
0.00
0.02
0.04
0.06
0.08
6500
7000
7500
8000
8500
λ(Å)
CH2
CH2
CH2
CH2
H2C
H2C

TABLE 1

THE OBSERVED BAND MAXIMA FOR THE CH-STRETCHING OVERTONE SPECTRA OF SEVERAL ALKANES (cm^{-1})

Molecule	Assignment	$\Delta v_{CH} = 2$	$\Delta v_{CH} = 3$	$\Delta v_{CH} = 4$	$\Delta v_{CH} = 5$	$\Delta v_{CH} = 6$
propane	CH_3		8423[a]	10958	13382	15748
n-butane	CH_3		8436[a]	10963	13392	15748
n-butane	CH_2				13156	
n-pentane	CH_3		8396	10958	13387	15726
n-pentane	CH_2		8275	10765	13158	
n-hexane	CH_3		8392	10948	13378	15708
n-hexane	CH_2		8268	10769	13151	15394
n-heptane	CH_3		8389	10937	13365	15686
n-heptane	CH_2		8266	10767	13144	15375
isobutane	CH_3			10956	13383	15726
isobutane	CH			10643		
2-methylbutane	CH_3		8401[a]	10964	13403	15723
3-methylpentane (l)	CH_3	5879	8408	10970	13423	15731
3-methylpentane (s)	CH_3		8408	10983	13450	15830
cyclohexane	CH_2			10816	13218	
cyclohexane	CH_2			10694		

a) one measurement only

parameters x_1, x_2 and $2/x_3$ (=FWHM), are given in Table 2. An example of a typical deconvolution set is given in figures 26, 27 and 28 and represents the work done on n-heptane. Experimental data, digitized and converted by program PC-138, have been plotted in these illustrations and under each band envelope are approximations of the Lorentz peaks calculated from the parameters generated by the deconvolution program. The straight line, running horizontally beneath each band envelope, is the baseline, also generated by the program. Figure 29 is a similar plot for $\Delta v_{CH} = 4$ of isobutane and is given as an illustration of some of the difficulties in the deconvolution.

A visual comparison of experimental and calculated results was often done by plotting the respective band envelopes. A sample of this kind of comparison is given in figure 30 for the $\Delta v_{CH} = 5$ overtone of n-heptane. The deconvolution of the $\Delta v_{CH} = 5$ overtone of n-heptane, given in figure 30, resulted in the poorest fitting calculated band envelope, on the basis of a final value of FM (the maximum ordinate difference) of 0.08 transmittance units. For all other deconvolutions the value of FM at termination was in the range of 0.01 to 0.05 transmittance units. The average values of FM were 0.04, 0.02 and 0.04 transmittance units for $\Delta v_{CH} = 3$, 4 and 5 respectively. The position of the maximum difference, as given by WFM, was generally found in the tails of the curves. A probable reason for the observed discrepancies between experimental and calculated results at the extremities of the band envelopes is the broadening of the peaks by intermolecular interactions, resulting in non-Lorentzian lineshapes. The possibility of non-Lorentzian lineshapes will be discussed further in the Appendix.

THE UNIVERSITY OF MANITOBA LIBRARIES

Fig. 26 An illustration of the calculated local mode components of the $\Delta v_{CH} = 3$, CH-stretching overtone band of n-heptane. (·····) Experimentally observed overtone band; (═══) Lorentzian peaks, calculated with parameters from a deconvolution program, representing each of the predicted pure CH local mode overtones and local mode combination bands.

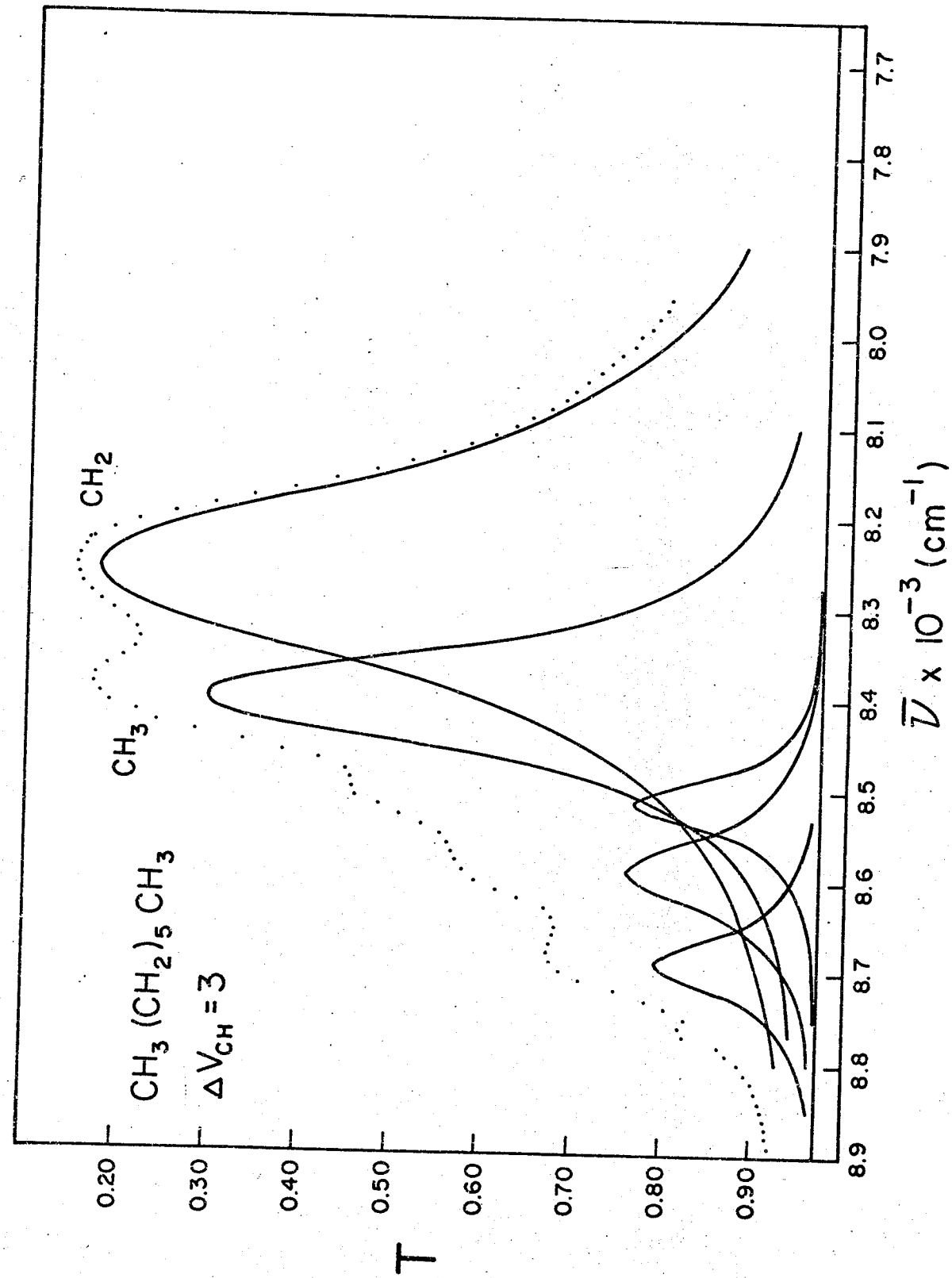
$CH_3(CH_2)_5CH_3$
$\Delta V_{CH} = 3$
CH_2
CH_3
T
0.20
0.30
0.40
0.50
0.60
0.70
0.80
0.90
8.9
8.8
8.7
8.6
8.5
8.4
8.3
8.2
8.1
8.0
7.9
7.8
7.7
$\overline{\nu} \times 10^{-3}$ (cm^{-1})

-43-

Fig. 27 An illustration of the calculated local mode components of the $\Delta v_{CH} = 4$, CH-stretching overtone band of n-heptane. (·····) Experimentally observed overtone band; (———) Lorentzian peaks, calculated with parameters from a deconvolution program, representing each of the predicted pure CH local mode overtones and local mode combination bands.

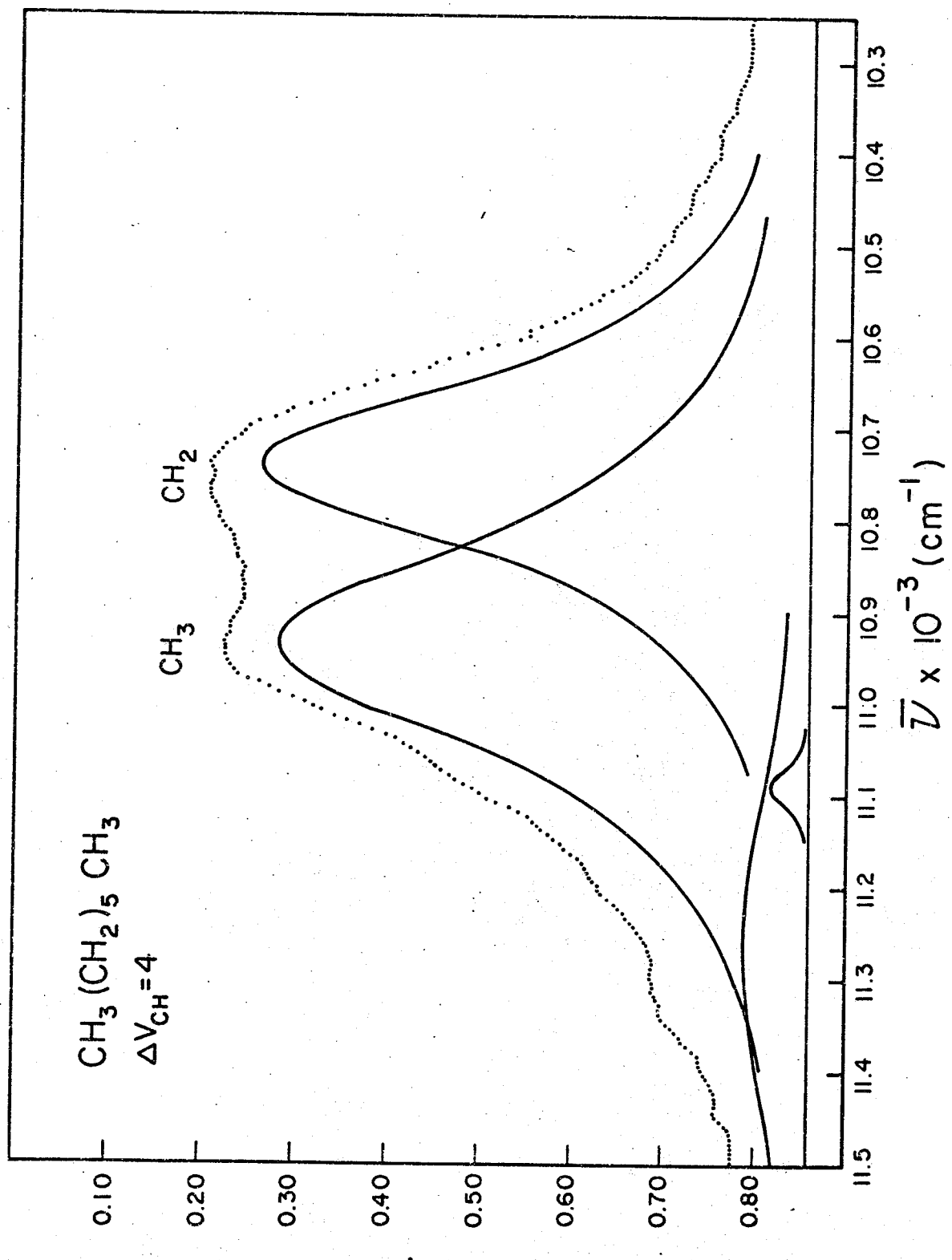
$CH_3(CH_2)_5CH_3$
$\Delta V_{CH}=4$
CH_2
CH_3
T
0.10
0.20
0.30
0.40
0.50
0.60
0.70
0.80
11.5
11.4
11.3
11.2
11.1
11.0
10.9
10.8
10.7
10.6
10.5
10.4
10.3
$\bar{\nu} \times 10^{-3}$ (cm^{-1})

Fig. 28 An illustration of the calculated local mode components of the $\Delta v_{CH} = 5$, CH-stretching overtone band of n-heptane. (·····) Experimentally observed overtone band; (———) Lorentzian peaks calculated with parameters from a deconvolution program, representing each of the predicted pure CH local mode overtones.

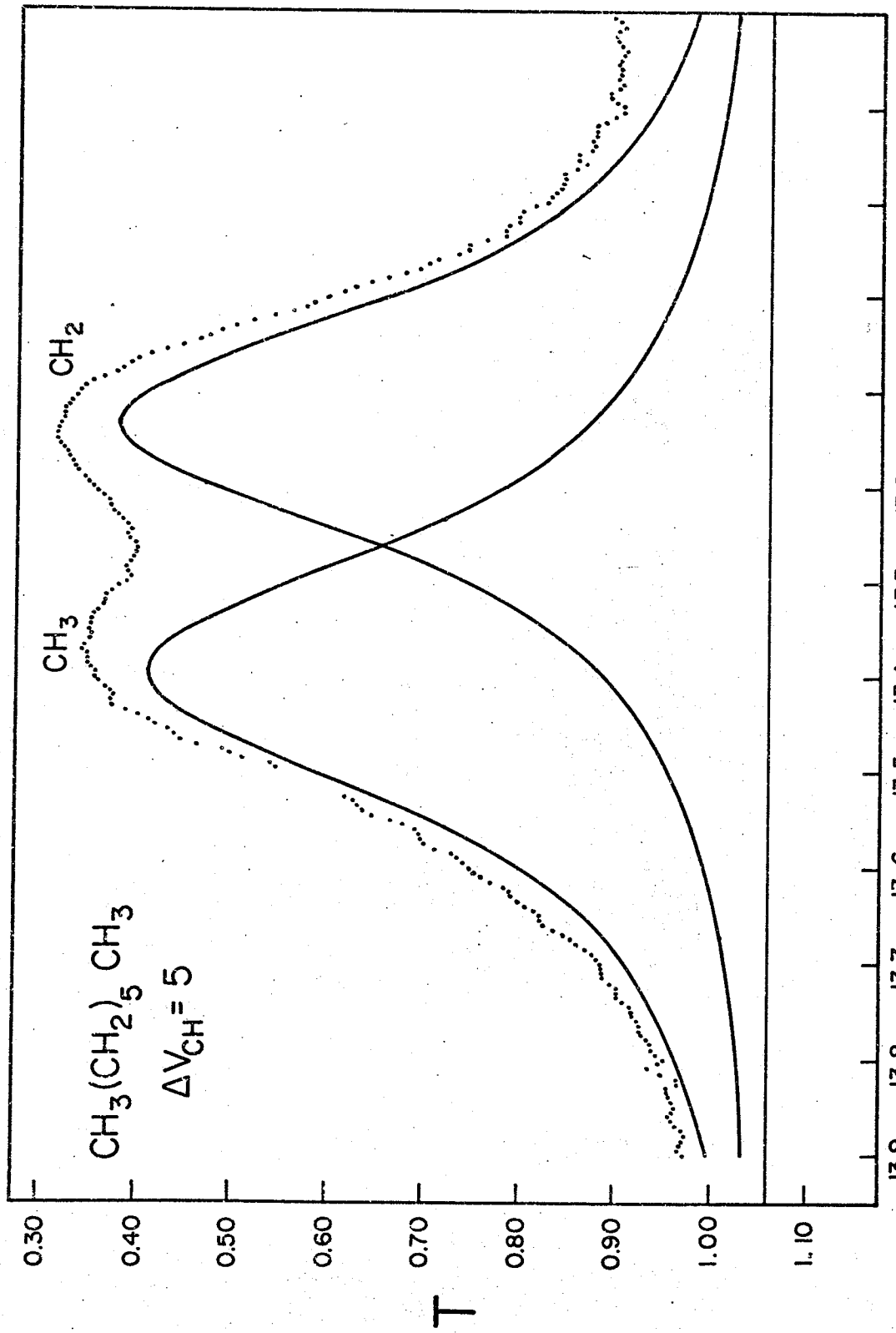
$CH_3(CH_2)_5\ CH_3$
$\Delta V_{CH} = 5$
CH_2
CH_3
T
0.30
0.40
0.50
0.60
0.70
0.80
0.90
1.00
1.10
13.9
13.8
13.7
13.6
13.5
13.4
13.3
13.2
13.1
13.0
12.9
12.8
$\overline{\nu} \times 10^{-3}\ (cm^{-1})$

-45-

Fig. 29 An illustration of the calculated local mode components of the $\Delta v_{CH} = 4$, CH-stretching overtone band of isobutane. (·····) Experimentally observed overtone band; (———) Lorentzian peaks, calculated with parameters from a deconvolution program, representing each of the predicted pure CH local mode overtones and local mode combination bands.

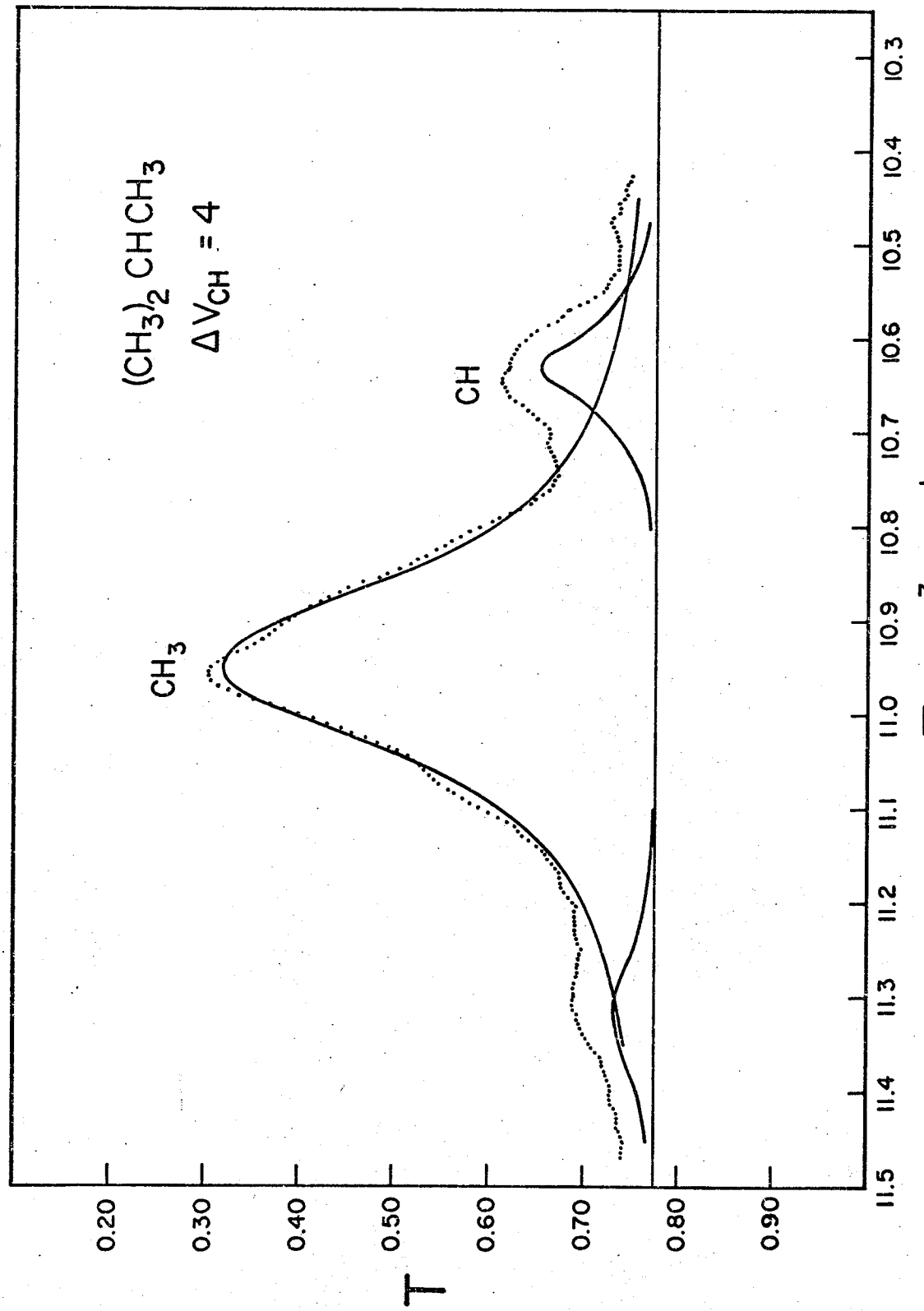
$(CH_3)_2 CHCH_3$
$\Delta V_{CH} = 4$
CH_3
CH
T
0.20
0.30
0.40
0.50
0.60
0.70
0.80
0.90
11.5
11.4
11.3
11.2
11.1
11.0
10.9
10.8
10.7
10.6
10.5
10.4
10.3
$\overline{\nu} \times 10^{-3}$ (cm^{-1})

Fig. 30 Calculated and observed CH-stretching overtone band of heptane corresponding to $\Delta v_{CH} = 5$. Calculated curve represents the sum of Lorentzian peaks, obtained from a computer assisted deconvolution of the experimentally observed overtone band.

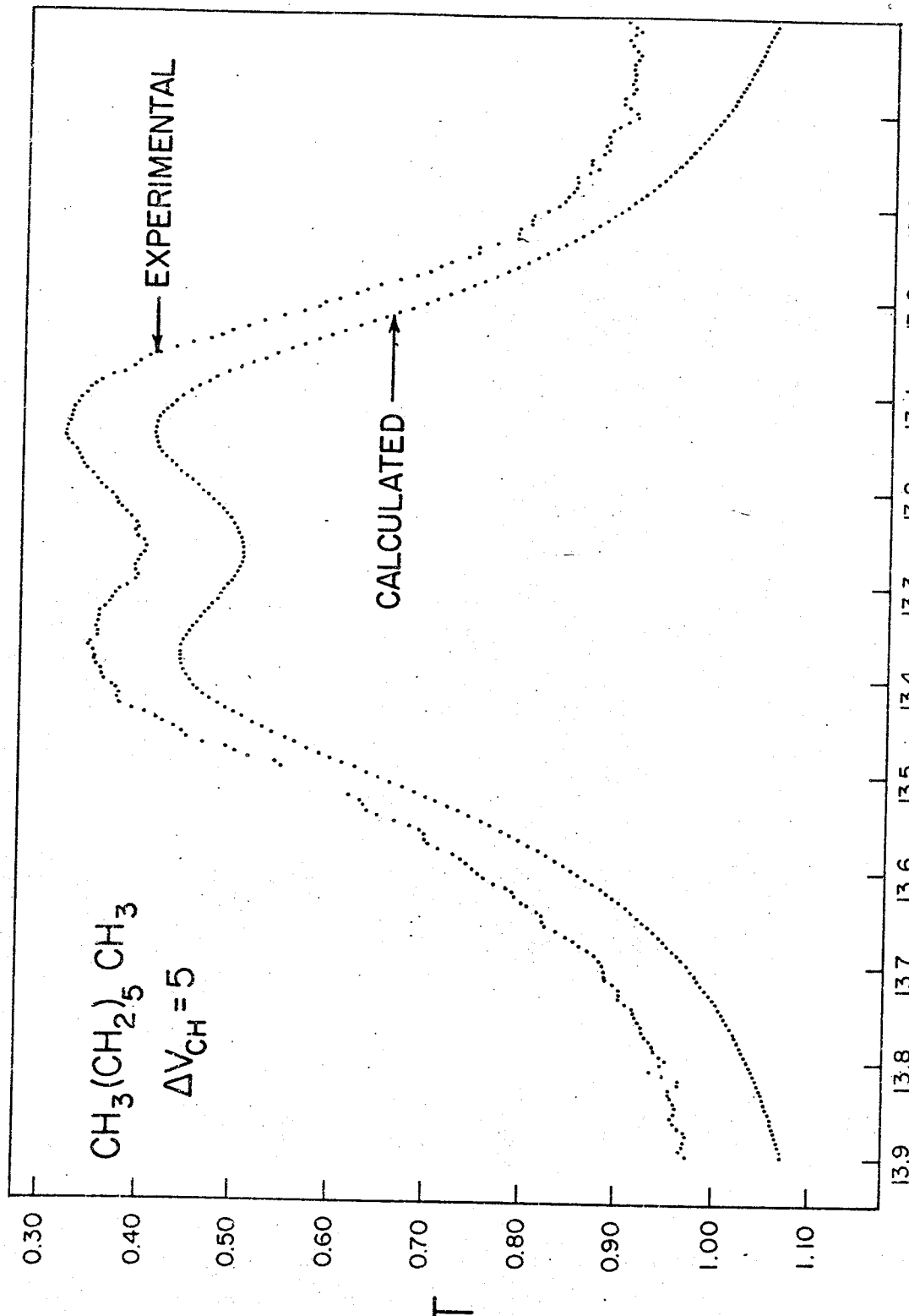
EXPERIMENTAL
CALCULATED
$CH_3(CH_2)_5\ CH_3$
$\Delta V_{CH} = 5$
T
0.30
0.40
0.50
0.60
0.70
0.80
0.90
1.00
1.10
13.9
13.8
13.7
13.6
13.5
13.4
13.3
13.2
13.1
13.0
12.9
12.8
$\overline{\nu} \times 10^{-3}\ (cm^{-1})$

TABLE 2

DATA OBTAINED FROM THE DECONVOLUTION OF THE CH-STRETCHING OVERTONE BANDS, Δv_{CH} = 3, 4 and 5, OF SOME ALKANES

			Local mode combination bands																
			I			II			III			CH_3			CH_2			CH	
Molecule	v_{CH}	n	x_1	x_2 (cm^{-1})	$2/x_3$ (cm^{-1})	x_1	x_2 (cm^{-1})	$2/x_3$ (cm^{-1})	x_1	x_2 (cm^{-1})	$2/x_3$ (cm^{-1})	x_1	x_2 (cm^{-1})	$2/x_3$ (cm^{-1})	x_1	x_2 (cm^{-1})	$2/x_3$ (cm^{-1})	x_1	x_2 (cm^{-1})	$2/x_3$ (cm^{-1})
propane	3	4	0.07	8701	97				0.05	8553	79	0.39	8426	91	0.17	8307	110			
n-butane	3	5	0.13	8721	73	0.11	8620	85	0.18	8550	34	0.92	8432	81	0.58	8295	117			
n-pentane	3	5	0.12	8692	79	0.12	8590	106	0.12	8515	58	0.65	8401	104	0.61	8262	176			
n-hexane	3	5	0.10	8692	76	0.11	8591	101	0.11	8518	61	0.59	8404	107	0.68	8263	178			
n-heptane	3	5	0.09	8690	75	0.11	8590	93	0.10	8515	67	0.52	8402	107	0.74	8260	183			
isobutane	4	3	0.03	11315	151							0.39	10948	187				0.08	10629	93
propane	4	3	0.04	11336	610							0.32	10956	187	0.11	10846	294			
n-butane	4	3	0.03	11312	493							0.31	10952	221	0.15	10755	183			
n-butane	4	4	0.03	11310	462				0.02	11103	39	0.31	10952	208	0.16	10759	191			
n-pentane	4	3	0.05	11318	517							0.58	10944	238	0.37	10746	181			
n-pentane	4	4	0.05	11304	501				0.03	11100	52	0.58	10945	216	0.39	10749	189			
n-hexane	4	3	0.05	11296	595							0.52	10942	241	0.44	10745	192			
n-hexane	4	4	0.05	11283	570				0.03	11095	58	0.52	10943	220	0.46	10748	198			
n-heptane	4	3	0.04	11241	612							0.49	10933	243	0.50	10740	176			
n-heptane	4	5	0.04	11264	519	0.004	11178	73	0.02	11092	48	0.49	10935	229	0.51	10741	179			
isobutane	5	2										0.36	13387	213				0.05	12960	249
propane	5	2										0.34	13400	248	0.05	13207	112			
n-butane	5	2										0.28	13397	248	0.14	13143	213			
n-pentane	5	2										0.51	13392	277	0.33	13134	226			
n-hexane	5	2										0.46	13385	275	0.39	13128	227			
n-heptane	5	2										0.41	13393	269	0.45	13133	244			

No attempt was made to deconvolute the $\Delta v_{CH} = 6$ overtones, since these bands were not of sufficient intensity to overcome the uncertainties due to background noise. It was found that, due to the nature of the data, the program wasn't able to sort out the smaller peaks consistently or often at all, especially when these peaks were nearby much larger peaks. For example, the CH peak position, for the branched alkanes 2-methylbutane and 3-methylpentane, was much too uncertain in trial computations and so the deconvolution of these compounds is omitted here.

Another result of the problem with smaller peaks was that the number of peaks assumed in a given overtone's deconvolution, n, was not uniform, especially for $\Delta v_{CH} = 4$. The $\Delta v_{CH} = 4$ region is interesting, because in that region the observed local mode CH-CH combination bands' intensities border on the limiting intensity that can be deconvoluted for this data. An increase in the number of CH_2 groups in the molecule, from propane to h-heptane, is observed to result in a respective increase in n from three to five, for $\Delta v_{CH} = 4$. Two of these peaks always represent the much more intense CH local mode overtones, corresponding to CH_3 and CH_2. The third, fourth and fifth peaks are local mode CH-CH combination bands and are observed just to the high energy side of the pure CH local mode overtone peaks. I believe that an increase in intensity of the local mode CH-CH combination bands, associated with the CH_2 hydrogen type, over the limiting intensity is responsible for the increase in n. An attempt to deconvolute a fourth peak, another local mode CH-CH combination band, for $\Delta v_{CH} = 4$ of propane gave ridiculous results, even though another small peak can clearly be

observed, at about 9025Å, as a shoulder on the main peak (figure 8). Thus, that peak was just too low in intensity to be isolated, due to only two contributing CH_2 hydrogens in the molecule. For $\Delta v_{CH} = 4$, the results of deconvoluting the band as both three and four (five for n-heptane) peaks are given, when possible. Comparison of these results provides a further illustration of the effects of smaller peaks on deconvolution. In general, however, the maximum number of peaks, which could be successfully deconvoluted from the band, were assumed and the results given in Table 2.

Table 3 presents the separation of CH_3 and CH_2 peaks for $\Delta v_{CH} = 3$, 4 and 5, as calculated from Table 2 data. The results for propane are observed to differ from those given for the other molecules, probably as a result of the increased inaccuracy of the deconvolution of smaller peaks. The average separation given for each Δv, therefore, excludes the results of propane.

Equation 2 was used to calculate the CH_3 type CH-stretching diagonal local mode anharmonicity constants from the experimentally observed CH_3 maxima of Table 1. The anharmonicity constants comprise Table 4. Hereafter, unless otherwise specified, any discussion of anharmonicity constants will refer to CH-stretching diagonal local mode anharmonicity constants, X_{11}.

It was originally hoped that deconvolution of the overtone bands would result in a refinement of the previously calculated CH_3 anharmonicity constants. However, the values obtained, using Table 2 deconvoluted peak maxima, were not any more uniform and the correlation coefficients often poorer. The deconvolution procedure did give CH_2

TABLE 3

SEPARATION OF THE CH_3 AND CH_2 PEAKS FOR THE ALKANE OVERTONES (cm^{-1})

Molecule	$\Delta v_{CH} = 3$	$\Delta v_{CH} = 4$	$\Delta v_{CH} = 5$
propane	120	110	193
n-butane	137	193	254
n-pentane	139	196	258
n-hexane	141	195	257
n-heptane	142	194	260
average	140	195	257

TABLE 4

RESULTS OF CH_3 ANHARMONICITY CALCULATIONS

FROM OBSERVED CH_3 PEAK MAXIMA

Molecule	X_{11} (cm^{-1})	ω_1 (cm^{-1})	r(a)
propane	-61.3	2988	-0.9980
n-butane	-62.4	2995	-0.9979
n-pentane	-60.6	2981	-0.9999
n-hexane	-60.1	2977	-0.9999
n-heptane	-60.7	2977	-0.9999
3-methylpentane	-60.1	2984	-0.9999
2-methylbutane	-59.7	2979	-0.9999
isobutane	-59.0	2974	-0.9976

(a) see text

peak maxima and so permitted the calculation of CH_2 anharmonicity constants. Both the CH_3 and CH_2 anharmonicity calculation results, from the deconvolution data, are presented in Table 5.

X_{11} calculations were usually based on four points, $\Delta v_{CH} = 3$ through 6. The exceptions, CH_2 anharmonicity constants for propane, n-butane, and n-pentane, are indicated in Table 5. Since the $\Delta v_{CH} = 6$ bands were not deconvoluted, the $\Delta v_{CH} = 6$ rough maxima were used in the X_{11} calculations. Although the CH_3 peak is always resolved in the $\Delta v_{CH} = 6$ region, the CH_2 peak was often of insufficient intensity, especially for the shorter chain compounds, to be resolved and so was unavailable for propane, n-butane and n-pentane. Where four points were available, little change was observed in the CH_2 anharmonicity constants if only three points were used in the calculation, that is when $\Delta v_{CH} = 6$ is omitted. Therefore, it is believed that the values, calculated from only three points, are comparable. The value of $-68.0\ cm^{-1}$, found for the CH_2 anharmonicity constant of n-butane is too high, relative to the X_{11}'s of the other alkanes. The erroneous value probably reflects the increased inaccuracy of the deconvolution of the smaller CH_2 peaks.

Dissociation energies were calculated for two of the types of CH oscillator present in alkanes, that is CH_3 and CH_2. An equation, relating the dissociation energy of a Morse oscillator to its anharmonicity constant, X, and harmonic frequency, ω, was used for the calculation. Further details of the calculation of these dissociation energies is presented in the Discussion section of this thesis. The calculated dissociation energies are listed in Table 6 and are

TABLE 5

RESULTS OF THE CH_3 AND CH_2 ANHARMONICITY CALCULATIONS

FROM THE DECONVOLUTED PEAK MAXIMA

Molecule	CH_3			CH_2		
	X_{11} (cm^{-1})	ω_1 (cm^{-1})	r	X_{11} (cm^{-1})	ω_1 (cm^{-1})	r
propane	-61.1	2988	-0.9984	-64.0[a]	2963	-0.9980
n-butane	-61.7	2991	-0.9975	-68.0[a]	2967	-0.9982
n-pentane	-60.4	2980	-0.9998	-63.5[a]	2943	-0.9995
n-hexane	-61.4	2984	-0.9998	-62.1	2939	-0.9996
n-heptane	-61.6	2984	-0.9993	-62.8	2940	-0.9996

(a) calculated using only 3 pts,, Δv_{CH} = 3, 4 and 5, because no Δv_{CH} = 6 point available.

TABLE 6

A COMPARISON OF CALCULATED AND LITERATURE DISSOCIATION ENERGIES FOR CH_3 AND CH_2 TYPE C-H BONDS

Hydrogen Type	Calculated Dissociation Energy	Kinetically Determined Dissociation Energy(a)
CH_3 (primary)	104 Kcal	98 Kcal
CH_2 (secondary)	99 Kcal	95 Kcal

(a) References 24, 26, 27, 28

compared to accepted, kinetically determined values.

The purpose of Table 7 is to compare the CH_3 anharmonicity constants, calculated for solid (77°K glass) and liquid 3MP. An illustration of the results is also presented, pictorially, in figure 31, by a plot of $\Delta E/v$ versus v for both of these phases of 3MP. The data, used to calculate the X_{11}'s, was taken from Table 1. As shown by a comparison of the values in Tables 4 and 5, convolution of the usually predominant CH_3 peak with other peaks, such as CH_2, results in only a slight shift in the CH_3 peak position. Since the shift is generally less than the errors inherent to the deconvolution, the CH_3 peak maxima of Table 1 are sufficient for a comparison of the CH_3 anharmonicities of solid and liquid 3MP.

Fig. 31 A plot of Equation 2 for the CH_3 transitions from the experimental solid (77°K glass) and liquid (room temperature) spectra of 3-methylpentane in the region $\Delta\nu_{CH} = 3$ to $\Delta\nu_{CH} = 6$.

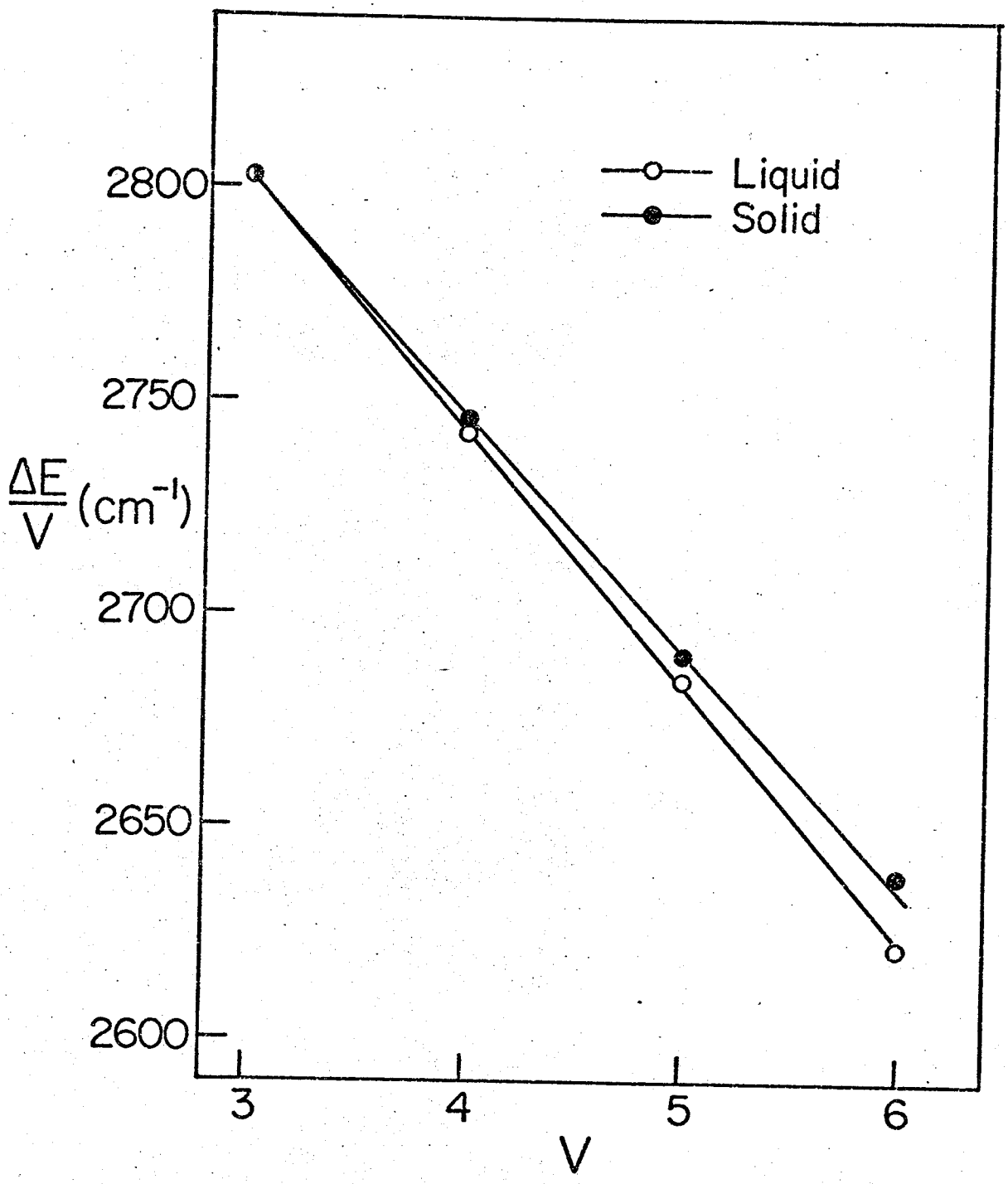
Liquid
Solid
2800
2750
2700
2650
2600
ΔE/V (cm⁻¹)
3
4
5
6
V

TABLE 7

DIAGONAL LOCAL MODE ANHARMONICITY CONSTANTS FOR THE CH_3 TRANSITIONS IN 3-METHYLPENTANE

Phase	X_{11} (cm^{-1})	r(a)
Liquid	-60.1	-0.9999
Solid	-54.8	-0.9998

(a) see text

DISCUSSION

A. The Local Mode Character of CH-Stretching Overtone Spectra

The alkane spectra obtained in this study have been presented almost in their entirety, because of the dramatic way that the complete set illustrates the local mode character of CH-stretching overtone spectra. The most natural interpretation of these spectra, especially for the higher overtone bands, is that each band is constructed of several peaks, each one representing a different hydrogen type. The variation of peak size with respect to the number of oscillators of one type bears a great similarity between these spectra and wide band NMR.

i) Nonequivalent CH Groups

Throughout the alkane spectra, the resolution of CH_3 and CH_2 peaks is evident, the CH_3 peak appearing at higher energy. The alkyl CH_3 local mode peaks' ΔE's, given in Table 1, are remarkably similar to those previously observed for the methyl groups of toluene and the xylenes (11), especially when one considers the difference in environment of these methyl groups. The average of the reported CH_3 values of toluene and the xylenes are 8378, 10959, 13409 and 14798 cm^{-1} for Δv_{CH} = 3, 4, 5 and 6 respectively. An additional peak is observed at even lower energy for the branched alkanes and this peak is due to the tertiary CH bond at the branch point. For isobutane, an alkane with no CH_2 hydrogens, it is readily observed as an isolated peak in figures 13 and 22. The relative energies of the three types of peak qualitatively follows the trend of decreasing bond strength. A tertiary CH bond is, for example, the weakest of the three, due to the effects of

increased carbon substitution.

The above assignments are also supported by the readily observed correlation of peak size to the number of oscillators of a given type of nonequivalent CH group. The CH_2 peak, which progresses from a shoulder in propane to a clearly resolved peak in n-heptane, clearly reflects the stepwise increase in the number of CH_2 groups as the alkane carbon chain lengthens. Similarly, a comparison of the branched chain alkane to straight chain alkane spectra reveals an increase in the CH_3 peak resulting from three additional CH_3 type hydrogens in the branched compounds.

It is interesting to note that a similar correspondence is found in the normal mode-local mode combination bands observed in the spectral region between the pure local mode overtones. These bands, as previously stated, have been attributed to the multiple excitation of a local CH oscillator with the addition of one quantum of a lower frequency normal mode (4). They are observed to show a parallel structure to that of their parent band. For example, the bands to the low energy side (8000-8500Å) of the pure local mode band in the $\Delta v_{CH} = 5$ spectra (figures 17-25), are combination bands involving the $\Delta v_{CH} = 4$ local mode plus one quantum of a lower frequency normal mode. These normal mode-local mode combination bands reflect not only the doublet (or triplet) structure of the parent CH-stretching local mode overtone, but also the relative intensities of the component peaks. The parallel nature of the normal mode-local mode combination band structure supports the local mode interpretation of these bands.

ii) Other Local Mode Characteristics

The alkane spectra presented are striking in their similarity. For each overtone transition, the only variation appears to be the relative increase or decrease of certain peaks of the different compounds, corresponding with the number of hydrogens represented by the peak.

A comparison of the bandwidths of each overtone band reveals they are quite invariant from molecule to molecule. The bandwidths are small and comparable to those previously observed for CH-stretching overtones. The overtone bands also become more complex towards the lower overtones, primarily due to an increase in the number and intensity of local mode CH-CH combination bands. For $\Delta v_{CH} = 5$ only a slight broadening of the high energy side of the pure local mode overtone suggests the presence of combination bands. In the $\Delta v_{CH} = 4$ spectra, in addition to the broadening of the pure overtone, a single well resolved combination band is observed. By $\Delta v_{CH} = 3$, three perceptible bumps, each one a combination band, are generally observed to the high energy side of the pure CH local mode peaks. These features, a consistent narrow bandwidth and increased complexity towards the lower overtones, are not expected in terms of normal modes.

To further the discussion of the differences between the experimentally observed CH-stretching overtone spectra and the expectations of a normal mode analysis, Figure 32, obtained from the paper on dichloromethane (4), has been introduced. Spectra A and B are comparisons of two different calculated band envelopes (dotted lines) to the experimentally obtained $\Delta v_{CH} = 4$ overtone transition of liquid phase

Fig. 32 Taken from Figure 5 of reference 4, copyright Academic Press. Calculated and observed $\Delta v_{CH} = 4$, CH-stretching overtone spectra of dichloromethane. (A) (-----) Calculated curve based on anharmonic normal mode components; (———) low resolution experimental spectrum; (B) (-----) computed spectrum of overtones and combinations of the modes with frequency and anharmonicity 2991 (-55), 2991 (-55) and 1429 (0) cm^{-1} with a weighting of the fundamental local-mode overtone 50 times that of a combination band of the same degeneracy. All computed components were assigned a bandwidth of 80 cm^{-1}.

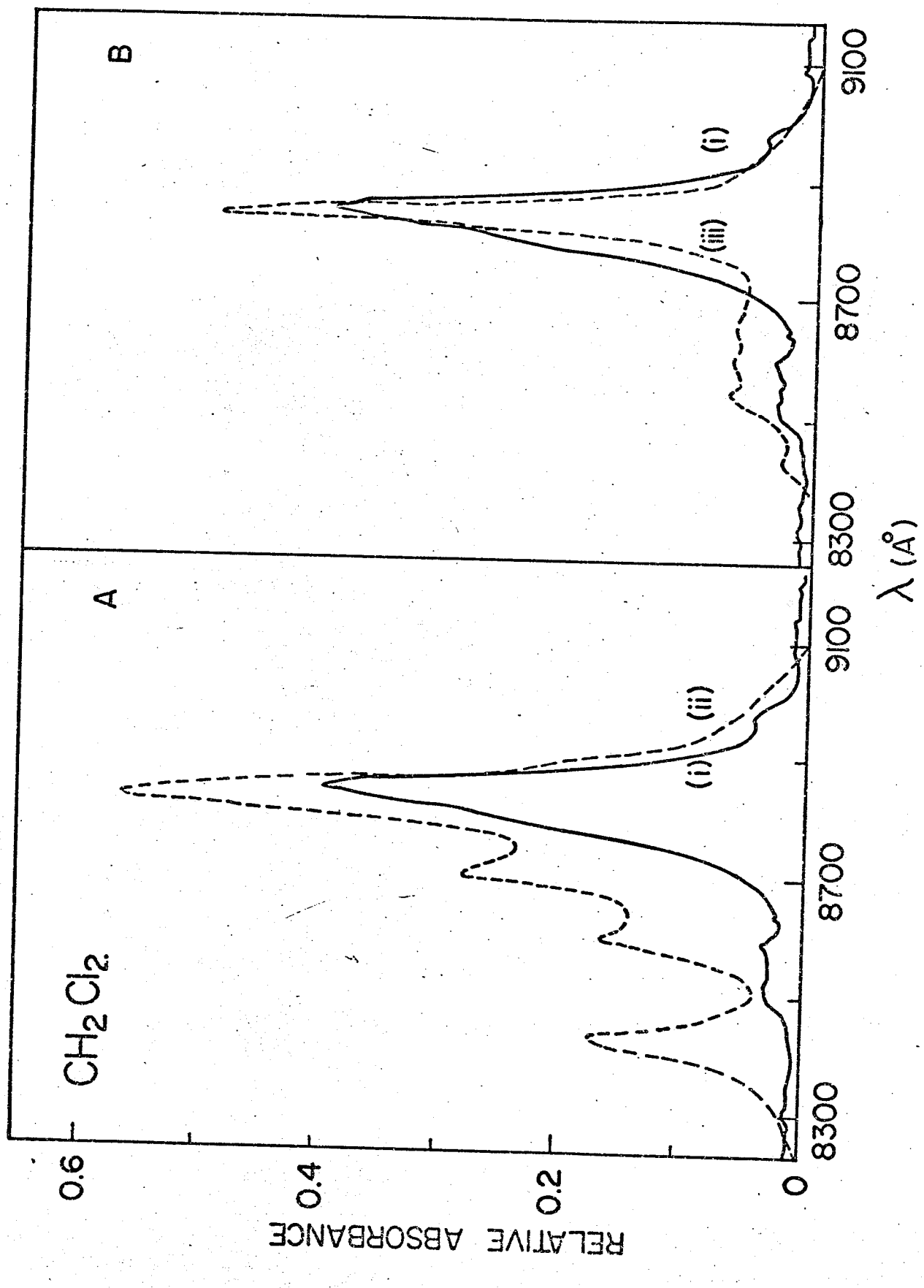
RELATIVE ABSORBANCE
0.6
0.4
0.2
0
8300
8700
9100
λ (Å)
A
B
CH_2Cl_2
(i)
(ii)
(iii)

dichloromethane. The calculated spectrum A represents the anharmonic normal mode representation of the CH overtone band. Numerical values were obtained for the normal mode anharmonicity constants and these were used to calculate the energies of the normal mode components of the overtone band. The components were then weighted with respect to their anharmonicities and the calculated curve was obtained as the sum of Lorentzian bands, each representing a single component.

Calculated band B was produced on the basis of the local mode model. A computer program, using a state counting algorithm described by Beyer and Swinehart and modified to include anharmonic effects by Stein and Rabinovitch,(23) was used to generate all possible combination and overtone states of the two CH local modes and a single harmonic CH bending normal mode. Components corresponding to pure CH local modes, that is all the energy in a single CH oscillator, were weighted 50 times. Lorentzian bands were again centered around each component and summed.

Several forementioned points are clearly illustrated by a comparison of these calculated curves to the experimentally observed CH-stretching overtone spectra of dichloromethane. The overtone band, calculated on a normal mode basis, is more complex or broader than the observed CH-stretching overtone band. Extra structure is predicted to higher energy than the observed overtone band and represents the contributions of some of the less anharmonic normal modes.

Even the presence of local mode CH-CH combination bands does not widen the observed overtone band to the width predicted by normal modes. Although these combination bands represent a normal mode influence, it

is obvious from figure 32 that their intensity is much less than that of the contributions, predicted on the basis of anharmonically coupled normal modes, of the more harmonic normal mode components. Even in the local mode analysis, it was necessary to weight the pure CH local modes fifty times at $\Delta v_{CH} = 4$ and two hundred times at $\Delta v_{CH} = 5$, relative to combination bands, to obtain comparative bandshapes. The increasing weight of pure CH local modes relative to combination bands at the high overtones is noted in the experimental alkane spectra as the observed decrease, from $\Delta v_{CH} = 3$ to 5, of the contributions of local mode CH-CH combination bands. Comparison of the observed alkyl normal mode-local mode combination bands shows that these bands also fall off in intensity at a much faster rate than the pure CH local mode bands.

In terms of normal modes the opposite trend is predicted. A calculation of the overtone band for the $\Delta v_{CH} = 5$ transition of dichloromethane, on the basis of anharmonically coupled normal modes, resulted in an even broader and more complex band due to an increase in the number of allowed states. Furthermore, dichloromethane is a relatively simple molecule, when compared to the alkanes studied here. For larger molecules the number of allowed normal mode states increases even more rapidly as v increases. An example is benzene for which there are 3 symmetry allowed normal mode states at $\Delta v_{CH} = 2$ and 75 (doubly degenerate) normal mode states for $\Delta v_{CH} = 6$. Thus, the complexity of higher overtones for larger molecules, such as the longer chain alkanes, is predicted by a normal mode analysis to be even greater. Also, the large differences in size and structure of the alkanes studied should

be reflected, in normal mode terms, by a corresponding difference in the number of allowed states. The observed consistency of bandwidth, for each overtone, does not support this concept.

In terms of local modes, the observed local spectral features are the result of states in which all vibrational quanta are localized in a single CH bond. The increasing complexity towards the lower overtones is required for a convergence to the traditional normal mode overtone pattern. The observed CH-stretching overtone spectra cannot be readily explained in terms of normal modes, but fall simply and naturally into a local mode description.

B. DCON - The Deconvolution Study

Most of the data obtained from the deconvolution of the overtone bands, Δv_{CH} = 3 to 5, of the straight chain alkanes are summarized in Table 2. Here again the peaks, represented by their parameters, are seen to form very consistent sets, especially for those compounds for which the experimental conditions were the same. (e.g. n-pentane, n-hexane, and n-heptane).

i) Bandwidths

The narrowness of the bandwidths of pure local mode overtone peaks is clearly exemplified by the values of $2/x_3$, the FWHM. An increase in the bandwidth of approximately 45 cm^{-1} is observed, for both CH_3 and CH_2 peaks, on comparison of Δv_{CH} = 4 and Δv_{CH} = 5 results. The Δv_{CH} = 5 peak is the larger. However, although a bandwidth increase is also observed from Δv_{CH} = 3 to 4, it is quite different for the CH_3 and CH_2 peaks. The CH_3 peak changes significantly, but the CH_2 peak negligibly, in width from Δv_{CH} = 3 to 4. Comparison of these peaks in figures 27, 28 and 29 for n-heptane reveals the source of this difference. The CH_3 peaks and the CH_2 peaks, resulting from the deconvolution of Δv_{CH} = 4 and 5 overtones are comparable, but those found for Δv_{CH} = 3 are markedly different in appearance. The difference is the result of a greater increase in the intensity of local mode CH-CH combination bands at Δv_{CH} = 3, due to the increasing influence of normal modes. As previously explained in the Results section, at Δv_{CH} = 4, the local mode CH-CH combination bands border on the minimum intensity which can be accurately isolated by the deconvolution program. The increased intensity of these combination bands for Δv_{CH} = 3 makes them easier to isolate from

the larger pure local mode overtones, but for $\Delta v_{CH} = 4$ and 5, these rapidly decreasing peaks become increasingly difficult to separate. Therefore, I believe that the CH_3 and CH_2 peaks for $\Delta v_{CH} = 4$ and 5 are more comparable because of the failure of the deconvolution, for $\Delta v_{CH} = 4$ and 5, to resolve completely the local mode CH-CH combination bands hidden on the high energy side of the pure CH_3 local mode peak. The result is a broadening of the CH_3 peak to include these smaller, unresolved peaks and a subsequent, small reduction in the CH_2 peak bandwidth for $\Delta v_{CH} = 4$ and 5. Corroborative evidence is given by a comparison of the results (Table 2) obtained when the $\Delta v_{CH} = 4$ overtone was deconvoluted as both three andffour (or five) peaks for n-butane, n-pentane, n-hexane, and n-heptane. The resolution of the fourth peak, a local mode CH-CH combination band, is observed to decrease the FWHM of the CH_3 peaks by an average of 18 cm^{-1}. The CH_2 peaks' FWHM are increased by an average of 7 cm^{-1}. The observed changes in the FWHM illustrate the possible effects of unresolved combination bands.

Also related is the general trend of the $\Delta v_{CH} = 4$, CH_3 peaks to shift, after deconvolution, to a lower energy. These peaks, usually the most prominent, were expected to shift slightly outward, to a higher energy, or not to shift at all. Figure 29 illustrates this problem. Here the CH_3 peak of isobutane is obviously overweighted to compensate for an undeconvoluted peak at about 11100 cm^{-1}. The result of its extra breadth was a shift of its maxima to lower energy to obtain a best fit of the data.

A comparison of the CH_3 and CH_2 peak areas also supports the

overweighting of the CH_3 peaks, at Δv_{CH} = 4 and 5, to incorporate the smaller, unresolved local mode CH-CH combination bands. A rough correlation has been previously reported between the ratio of the peak areas and the ratio of the number of equivalent hydrogen for the Δv_{CH} = 5 bands of toluene and m-xylene. The area ratios were observed to be ≃ 2/1 and ≃5/7, aryl/alkyl respectively(11). For the deconvolution results of n-heptane, only the peaks calculated for Δv_{CH} = 3 are observed to have an area ratio near the CH_3/CH_2 hydrogen ratio of 6/10. Indeed, for Δv_{CH} = 4 and 5 the CH_3 peak is comparable, if not larger, in size to the CH_2 peak, suggesting again that it has been overweighted.

Although the FWHM increase for the pure local mode overtone peaks may not be consistent, or due in part to the problems of the resolution of smaller peaks, I believe that the overtone bands do broaden significantly with increasing v. A similar correspondence, although less pronounced, is generally observed between the alkane chain length and the FWHM. Both of these broadenings could be the result of a solution effect and increasing deviation from the Lorentzian bandshape. These ideas will be discussed further in the Appendix.

ii) Local Mode CH-CH Combination Bands

The increased importance of normal modes towards the lower overtones is also reflected by the increase from two to five in the number of peaks deconvolutable from each band. Local mode CH-CH combination bands, resulting from states in which the vibrational quanta are distributed in two bonds, are seen to progress from an undeconvolutable broadening of Δv_{CH} = 5 to three well-defined peaks for Δv_{CH} = 3. These three combination bands are labelled I, II and III in Table 2. The

increasing importance of these local mode CH-CH combination bands has previously been explained as representing a shift towards the normal mode pattern.

For $\Delta v_{CH} = 4$, the problem of the low intensity of these combination bands is again observed. The highest energy combination band at $\Delta v_{CH} = 4$, I in Table 2, is believed to represent at least two unresolved peaks, which accounts for the large FWHM.

A probable assignment of these local mode CH-CH combination bands is possible if one notes the correlation between the appearance of given bands and the structure, that is type of hydrogens present, for the compound for which the band is present. For example, isobutane cannot have any local mode CH-CH combination bands involving CH_2, due to the absence of this hydrogen type. Comparing the FWHM of I for the $\Delta v_{CH} = 4$ transition of isobutane to the other alkanes reveals that it is much narrower and so confirms the suspicion that, for the other compounds, it represents several, unresolved peaks. This result also indicates that the highest energy band, I, which is consistently visible in $\Delta v_{CH} = 3$ and 4 spectra, involves only CH_3 hydrogens. In other words, it represents a state in which the vibrational quanta are distributed in two of the CH bonds of a methyl group. A most probable distribution is one quantum in one bond and the remaining in a second. The fact that, for the straight chain alkanes, this peak, I, is nearly constant in x_1 and FWHM also suggests that it corresponds in character to a CH_3 local mode CH-CH combination band since the number of CH_3 hydrogens is also constant from molecule to molecule.

The other [illegible] combination bands are believed to involve

The other local CH-CH combination bands are believed to involve CH_2 hydrogens since they seem to be responsive to the number of CH_2 hydrogens in a given compound. They are distinctly absent from compounds with few or no CH_2 groups. The local CH-CH combination band, marked III in Table 2, most likely represents a state similar to the forementioned for CH_3, but here the quanta are distributed in two CH bonds of a CH_2 group. Combination band II cannot be as readily assigned, however given its absence for $\Delta v_{CH} = 3$ of propane and presence for $\Delta v_{CH} = 4$ of n-heptane, it also seems to be related to the CH_2 hydrogen, although not as strongly. A possible state which would have a weaker correspondence to the CH_2 hydrogens would result from the division of the vibrational quanta between two of the CH bonds of a neighbouring CH_3 and CH_2 group. Since the normal mode influence gains in importance about $\Delta v_{CH} = 3$, such a state is not unlikely. This possible assignment is corroborated by the significantly larger FWHM of combination band II as compared to I and III. The extra breadth would be due to the presence of the two unresolved transitions to the two combination states $2(CH_3)$, $1(CH_2)$ and $1(CH_3)$, $2(CH_2)$.

iii) Peak Separation

Table 3, besides indicating that problems exist in the propane deconvolution, also contains some additional, interesting information. The separation of the CH_3 and CH_2 peaks, for a given overtone, may be written as

$$E(CH_3)-E(CH_2) = v\,[\omega_1(CH_3)-\omega_1(CH_2)] + v^2[X_{11}(CH_3)-X_{11}(CH_2)] \qquad (3)$$

Equation 3 is obtained from the difference of the two equations, based on equation 2, written for CH_3 and CH_2. From equation 3, it can be seen

that the peak separation should show a nearly linear dependence upon v, if the correction due to the anharmonicity difference is negligible. Table 3 average separations do show an almost linear increase with v, as expected. Thus, if the peak separation is divided by v, the vibrational quantum number, the result should be a fairly constant value. The only change in this value will be due to the anharmonicity constants difference and should show a dependence upon v. Performing a division by v, on the average peak separations for Δv_{CH} = 3, 4 and 5, gives values of 47, 49 and 51 cm^{-1} respectively. These results upon solving equation 3, predict a difference in the harmonic frequencies, ω, of the order of 41 cm^{-1} and difference in the anharmonicity constants, X_{11}, of 2 cm^{-1} between CH_3 and CH_2 local modes. Comparison of the CH_3 and CH_2 values of X_{11} and ω_1, from Table 5, gives an average difference, neglecting the suspect n-butane results, of 2.0 and 38 cm^{-1} respectively. The validity of equations 2 and 3 for the alkane data reinforces the predictions that the local mode off-diagonal anharmonicity constants, the X_{ij}'s, are relatively small or tend to cancel relative to the X_{ii} terms.

The parameter ω^D_{CH} has been defined (171) as the fundamental CH-stretching frequency for a molecule with all the hydrogens but one replaced by deuterium. ω^D_{CH} should reflect the nature of an individual CH bond. The observed difference in the ω^D_{CH}'s for a hydrogen in a CH_4 environment from that for a CH_3 is approximately 50 cm^{-1}. A reasonable assumption is that a further change in environment, from CH_3 to CH_2, would result in a comparable change in the ω^D_{CH}. The value of 41 cm^{-1}, observed as the difference in harmonic frequencies of the two local

modes, agrees well with the separation predicted on the basis of ω^{D}_{CH}.

C. Anharmonicity Constants

Diagonal CH-stretching local mode anharmonicity constants, X_{ii}'s, are readily calculated via equation 2 and the peak maxima given in Tables 4 and 5. The calculated correlation coefficients, r, clearly illustrate the linearity of the $\Delta E/\tilde{\nu}$ plots. A value of -1.00 for a correlation coefficient indicates a perfect straight line with a negative slope.

i) Morse Oscillator

Substituents, not directly bonded to one of the atoms of a bond being homolytically broken, have been observed to have little effect on that bond's dissociation energy (24). Therefore, the dissociation energies of alkyl primary, secondary and tertiary hydrogens have been found to be characteristic of the respective hydrogen type, since the energy depends only on the number of alkyl groups bonded to the carbon of the CH bond. Table 5 shows that calculated X_{11} and ω_1 values are also distinct and fairly consistent for the various hydrogen types. Any deviations are readily accounted for in the experimental uncertainty. The local mode concept was originally derived from the analysis of larger amplitude CH vibrations, which correspond to dissociation at their limit. Thus the complimentary nature of dissociation energy and local mode parameters is to be expected. The applicability of the Morse oscillator, as a description of the local CH oscillator, has previously been demonstrated (16). The following relationship,

$$X = \omega^2/4D \qquad (4)$$

between the anharmonicity constant, X ($\equiv -x_e\omega_e$), and the dissociation energy, D, can be written if the Morse potential is a reasonable

approximation of the actual vibrational potential (25). Therefore, a further confirmation of the description of a set of weakly coupled anharmonic local oscillators in terms of a collection of Morse oscillators is expressed by the observed correspondence of anharmonicity constants and local mode frequencies with the dissociation energies.

ii) Dissociation Energies

Equation 4 was used to calculate dissociation energies, from experimentally obtained ω_1 and X_{11} values, for CH_3 and CH_2, that is, primary and secondary hydrogens. Comparison of these values with the accepted, kinetically determined, characteristic dissociation energies (24, 26, 27, 28), in Table 6, reveals that the calculated values are both somewhat high. However, the theory of the vibrations of a diatomic (29) gives an explanation for the discrepancy. These overestimations of D could result from the neglect of cubic and higher order terms in the derivation of equation 4. Birge-Sponer plots for a diatomic, in which the vibrational level spacing, ΔG, is plotted against the vibrational quantum number, v, to illustrate the increasing importance of these terms in higher v. The result is a downward curvature of such a plot for these higher vibrational levels. Since the dissociation energy is effectively the area under such a curve, an overestimation is expected if the cubic terms are omitted and the linear variance of ΔG with v assumed. A similar overestimation is probable for these results. Thus, the calculated dissociation energies are good estimates of the actual dissociation energy, considering the roughness of the data, and the applicability of equation 4 to a local CH oscillator is supported.

Comparison of the calculated values of X_{11} and ω_1 for CH_2 to the more consistent CH_3 results, via equation 4 and the respective kinetically determined dissociation energies, revealed that the calculated average values of the harmonic frequency and anharmonicity constant for CH_2 are a little high. The values given for n-hexane and n-heptane are found to be more reasonable, relative to the primary hydrogen results. In the observed spectra, the CH_2 peak is more prominent for n-hexane and n-heptane and so deconvolution would yield more accurate maxima and a better set of local mode parameters is expected. Optimized values for secondary hydrogens, calculated from the results of n-hexane and n-heptane exclusively, of $-62.5\ cm^{-1}$ and $2940\ cm^{-1}$ are proposed for X_{11} and ω_1 respectively.

iv) Medium Effects

Dellinger and Kasha have recently developed a theory of the intermolecular perturbation of molecular potentials (30) and a proposed application is to vibrations describable by a Morse potential. This work and others (15) have already shown that a collection of Morse oscillators is a reasonable description of a set of loosely coupled anharmonic local oscillators and so such considerations should be applicable to the local CH-stretching oscillator.

The theory proposes that for such a system the solvent cage acts as a viscosity dependent barrier to dissociation (31). The potential, therefore, becomes more harmonic in a higher viscosity medium and this will be reflected by a decrease in the anharmonicity constant. Figure 33, from reference 31, provides an illustration of the change in anharmonicity of the higher vibrational potential predicted for higher viscosity media.

Fig. 33 The more harmonic potential (-----), resulting from the solid matrix perturbation of the original Morse potential (———) for the liquid phase. Adapted from Figure 1 of reference 31.

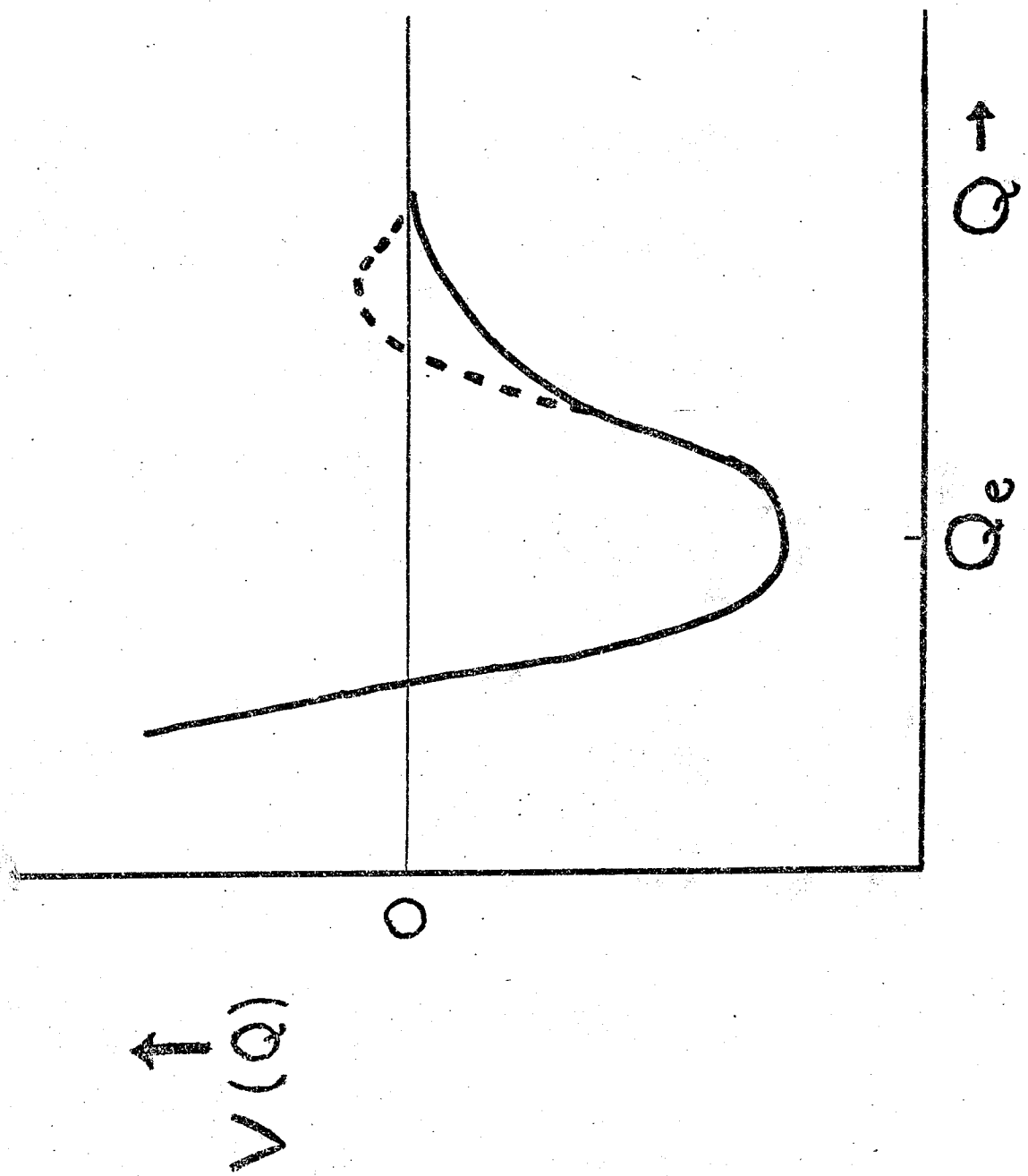
Q
Qe
O
V(Q)

3MP was chosen as a suitable system to test these ideas as its overtone spectrum is measurable in both the liquid phase at room temperature and as a clear rigid glass at 77°K. Analysis of the spectra allows calculation of the X_{11} from equation 2 and a direct comparison of the results for liquid and rigid media is possible.

The solid spectra showed about a 15% increase in intensity for the same pathlength due to a decrease in the volume on going to the glass. However, bandshapes remained very similar to those observed for liquid 3MP and therefore the solid 3MP spectra are not presented here. The CH_3 peak dominates each overtone band and so its position was assigned simply as the band maxima observed in the spectrum (see Table 1). As previously stated, comparison of deconvoluted and rough data for the CH_3 peaks reveals only slight shifts in the peak maxima and this is confirmed by the lack of any large, uniform changes in the calculated X_{11} values for CH_3, given in Tables 4 and 5.

Both solid and liquid plots of equation 2, given in figure 31, are almost perfect straight lines, as predicted by equation 2. The solid 3MP, $\Delta v_{CH} = 6$ point is the most uncertain, due to a small intensity on a rising background. The correlation coefficients, in Table 7, show the solid 3MP results to be only slightly poorer, but this is easily attributable to an observed noisier background.

Figure 31 clearly shows the difference in the slope that is representative of a difference in the anharmonicities of solid and liquid 3MP. As predicted, the anharmonicity of the more viscous solid phase is smaller than the liquid. Thus, intermolecular forces in the solid phase are directly shaping the vibrational potential

and rendering it more harmonic. The magnitude of this change, with X_{11} decreasing from -60.1 cm^{-1} to -54.8 cm^{-1}, is surprising, however, because the interaction of the solvent cage with the vibrations of the hydrogen atom might be expected to be minimal.

APPENDIX

Further Studies

This section has been added to allow some speculation about several puzzles that arose during this study for which no definite answers were obtained.

i) Cyclohexane

Of the CH-stretching spectra presented in this study, only those of cyclohexane (figures 16 and 25) do not conform with the local mode picture given thus far. Originally, cyclohexane was measured to be used as a reference, for the CH_2 group, in the computer deconvolution study. I had hoped to gain some information on the bandshape of the pure local mode overtone peaks from the cyclohexane spectra, since the one hydrogen type present was expected to give a single large peak. However instead, two major convoluted peaks were resolved for each overtone. In addition, the two observed peaks seem to lie to either side of the average CH_2 peak position, as if their position is weighted by their respective size. It did not seem probable that a peak of the size observed could be the result of the presence of an impurity in the sample, but to verify this conclusion a new, unopened bottle of spectro-grade cyclohexane was obtained. Samples from the new bottle were found to give identical results.

It is suggested that these two peaks represent the resolution of the axial and equatorial hydrogens of cyclohexane. On the vibrational time scale, the cyclohexane ring would be fixed and interconversion of the two hydrogen types stopped, allowing a discrimination of axial and equatorial hydrogens. If these peaks do represent axial and equatorial

hydrogens, then cyclohexane represents a further extension of the separation of nonequivalent hydrogens in CH-stretching overtone spectra. A study is presently underway to investigate this idea (32) and, if substantiated, will provide further support for the local mode interpretation of these spectra. The observed separation between the "axial and equatorial" CH-stretchings is about 110 cm^{-1} (from Table 1) at $\Delta v_{CH} = 4$ as compared to the CH_3 - CH_2 average separation of 195 cm^{-1} from Table 3.

ii) Bandshapes

Although a Lorentzian bandshape has been observed previously, for the $\Delta v_{CH} = 6$ overtone of gaseous benzene (17), there is some evidence in this study to suggest that there is also some Gaussian character in the overtone peaks. A majority of the alkanes studied were in the liquid phase and a Gaussian broadening of liquid phase spectra, due to intermolecular interactions, is probable.

A comparison of the observed and calculated $\Delta v_{CH} = 5$ overtones of n-heptane, given in figure 30, reveals that the experimental band is somewhat more round and broader than was predicted with pure Lorentzian peaks. The experimental spectrum does seem to be more Gaussian in shape. In fact, the termination of the iterations by slow convergence, for every deconvolution, indicates that the pure Lorentzian bandshape, assumed in the calculations, is probably not the real bandshape of the CH-stretching overtone peaks.

Experimentation with the fitting of single, isolated overtone peaks, using Lorentz-Gauss sum or product functions, would be instrumental in determining the exact bandshapes of the overtones. Since

cyclohexane has failed, as discussed above, to produce single, isolated peaks for each overtone, a possible choice for a reference compound would be neopentane, an alkane with only CH_3 hydrogens.

The Gaussian character of the overtones is not expected to be constant. Both the increase of vibrational quanta, Δv, and the length of alkane chain could increase the intermolecular interactions and subsequently the Gaussian contribution to a given peak. The increased Gaussian character is a possible explanation for the increased FWHM at higher v and for longer chained alkanes.

REFERENCES

1. B. R. Henry and W. Siebrand, J. Chem. Phys. 49, 5369 (1968).

2. R. J. Hayward, B. R. Henry and W. Siebrand, J. Mol. Spectrosc. 46, 207 (1973).

3. R. J. Hayward and B. R. Henry, J. Mol. Spectrosc. 50, 58 (1974).

4. R. J. Hayward and B. R. Henry, J. Mol. Spectrosc. 57, 221 (1975).

5. J. J. Fox and A. E. Martin, Proc. Roy. Soc. A175, 208 (1940).

6. T. Simanouti and S. Mizushima, J. Chem. Phys. 17, 1102 (1949).

7. J. K. Brown, N. Sheppard and D. M. Simpson, Discuss. Faraday Soc. 9, 261 (1950).

8. R. G. Snyder and J. H. Schachtschneider, Spectrochim. Acta 19, 85, 117 (1963).

9. M. Avanessoff and T. Gäumann, Helv. Chim. Acta 54, 995 (1971).

10. M. Avanessoff, H. D. Thang and T. Gäaumann, Helv. Chim. Acta 54, 1013 (1971).

11. R. J. Hayward and B. R. Henry, Chem. Phys. 12, 387 (1976).

12. M. Avanessoff and T. Gäumann, Helv. Chim. Acta 54, 1310 (1971).

13. R. L. Swofford, M. E. Long and A. C. Albrecht, J. Chem. Phys. 65, 179 (1976).

14. B. R. Henry and I. F. Hung, submitted for publication.

15. R. Wallace, Chem. Phys. 11, 189 (1975).

16. R. L. Swofford, M. S. Burberry, J. A. Morrell and A. C. Albrecht, J. Chem. Phys. 66, 5245 (1977).

17. R. G. Bray and M. J. Berry, personal communication.

18. S. A. Rice and W. M. Gelbart, Pure and Applied Chemistry 27, 361 (1971).

19. W. J. Potts, J. Chem. Phys. 20, 809 (1952).

20. R. J. Hayward, Ph.D. thesis--Polyatomic Anharmonicity: A Local Mode Approach to Overtone Spectra.

21. R. P. Young and R. N. Jones, National Research Council of Canada Bulletin No. 11, Ottawa 1968.

22. J. Pitha and R. N. Jones, National Research Council of Canada Bulletin No. 12, Ottawa 1968.

23. S. E. Stein and B. S. Rabinovitch, J. Chem. Phys. 58, 2438 (1973).

24. K. W. Eggers and A. T. Cocks, Helv. Chim. Acta 56, 1516 (1973).

25. W. Siebrand and D. F. Williams, J. Chem. Phys. 49, 1860 (1968).

26. J. A. Kerr, Chem. Rev. 66, 465 (1966).

27. D. M. Golden and S. W. Benson, Chem. Rev. 69, 125 (1969).

28. D. C. McKean, J. L. Duncan and L. Blatt, Spectrochim. Acta 29A, 1037 (1973).

29. G. Herzberg, Spectra of Diatomic Molecules (Van Nostrand, New York, N.Y., 1950).

30. B. Dellinger and M. Kasha, Chem. Phys. Letters 36, 410 (1975).

31. B. Dellinger and M. Kasha, Chem. Phys. Letters 38, 9 (1976).

32. I. F. Hung and B. R. Henry, unpublished work.